(Received 18 November 2025, Accepted 5 December 2025, Scheduled 12 January 2026)

An Overview of Advanced Control Technologies for Marine Propulsion Motors

Qingcheng Meng, Jingwei Zhu*, Yonghan Liu, Shukuan Zhang, and Yechi Zhang

College of Marine Electrical Engineering, Dalian Maritime University, Dalian, China

ABSTRACT: With the ongoing transformation of the global energy structure and growing demand for environmental sustainability, transportation electrification has been rapidly advancing and is becoming a key pathway toward achieving carbon neutrality. Maritime transportation accounts for a significant share of carbon emissions, and conventional fuel-based propulsion remains dominant. Consequently, marine electrification is experiencing a transformative opportunity driven by both energy and environmental imperatives. As the core component of the propulsion system, the electric motor places increasingly stringent requirements for control performance and reliability. This study reviews recent advances in marine propulsion motor control technologies, focusing on three major areas: model predictive control (MPC), fault-tolerant control (FTC), and position sensorless control. In MPC, multi-plane modeling and virtual voltage vector regulation for six-phase permanent magnet machines have substantially improved the dynamic response and control accuracy. Additionally, multi-objective optimization can be achieved through the design of weight factors, whereas the introduction of observers or data-driven approaches can enhance robustness against parameter variations. In FTC, the development from optimal current compensation to post-fault subspace reconstruction topologies has provided a theoretical foundation for robust control under complex operating conditions. In position sensorless control, medium- and high-speed sliding-mode observation combined with low-speed high-frequency signal injection enables accurate position estimation over the full speed range. Future research is expected to integrate the feature extraction and modeling capabilities of machine learning to enhance observer design and fault-tolerant strategies, promoting the intelligent and data-driven evolution of marine propulsion motor control technologies.

1. INTRODUCTION

With the ongoing transformation of the global energy structure and increasing awareness of environmental protection, transportation electrification has become one of the major development trends in the global transportation industry. Transportation electrification is not only an effective approach to address the growing challenges of energy crises and environmental pollution, but also a key technology for achieving sustainable development. Significant progress has been made in the electrification of road transportation, rail transit, and aerospace, where the adoption of green and clean energy sources is gradually replacing traditional fossil fuels, contributing to the reduction in greenhouse gas emissions and carbon footprints. However, in the maritime transportation sector, conventional fuel-powered ships still dominate, despite facing similar energy and environmental challenges. As the international community places greater emphasis on reducing marine pollution and achieving carbon neutrality, marine electrification is increasingly becoming a focal point and a key driver of industry transformation. In the field of marine propulsion, the development to date can be broadly categorized into two main types of propulsion systems.

1.1. Gear-Driven Propulsion

The "prime mover-gear transmission-propeller" configuration has been widely adopted in marine propulsion systems, where the prime mover is primarily a conventional diesel engine, as illustrated in Fig. 1. This traditional architecture offers several advantages, including technological maturity, extensive maintenance experience, high power density, long endurance, and strong adaptability to harsh marine environments. However, it also suffers from significant drawbacks such as environmental pollution, low energy efficiency, high noise and vibration levels, and elevated maintenance costs, which limit its sustainability in modern green shipping applications [1].

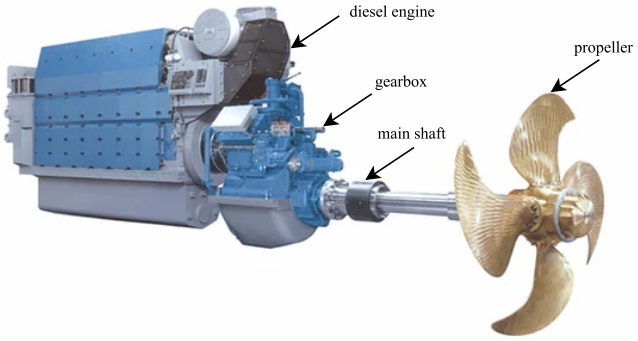

FIGURE 1. Diesel engine-gear transmission-propeller assembly diagram.

To address the aforementioned issues, the "electric motor-gear transmission-propeller" configuration has gradually attracted increasing attention as an alternative solution for marine propulsion [2], as illustrated in Fig. 2. Compared to the conven-

* Corresponding author: Jingwei Zhu (zjwdl@dlmu.edu.cn).

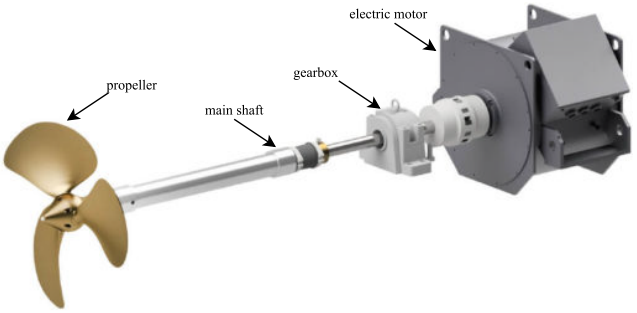

FIGURE 2. Electric motor-gear transmission-propeller assembly diagram.

tional "prime mover-gear transmission-propeller" system, the electric motor provides a cleaner and more efficient propulsion approach. By utilizing electrical energy as the driving source, the electric motor significantly reduces the dependence on fossil fuels, thereby lowering greenhouse gas emissions and harmful pollutants to meet increasingly stringent environmental regulations [2].

Moreover, electric propulsion systems produce lower noise and vibration levels than traditional diesel engine systems. This not only improves the onboard working environment for crew members but also minimizes mechanical wear and structural fatigue, enhancing the vessel's long-term durability and reducing overall operating costs. With the growing adoption of renewable energy sources, electric propulsion systems can also be flexibly integrated with wind, solar, and other clean energy technologies, further strengthening the sustainability of marine transportation. Therefore, the "electric motor-gear transmission-propeller" configuration demonstrates distinct advantages in environmental performance, energy efficiency, noise reduction, and maintenance economy, representing a crucial direction for the transition toward green and sustainable shipping.

1.2. Integrated Direct-Drive Propulsion

With the advancement of cutting-edge technologies and renewed understanding of marine propulsion motors, two types of electric direct-drive propulsion systems have been developed: the podded propulsor and the rim-driven thruster. Both configurations eliminate the intermediate gear transmission mechanism and are characterized by a high degree of integration.

The podded propulsor is a type of direct-drive propulsion system that integrates the propulsion unit and power source into a pod structure located beneath the ship hull [3], as illustrated in Fig. 3. The core concept of this technology is the integration of the electric motor and propeller into a single unit, eliminating the need for shafts, gearboxes, and other mechanical transmission components. Originating in the 1970s and reaching commercialization in the 1990s, the podded propulsion system offers several advantages, including reduced spatial requirements, enhanced maneuverability with full 360° azimuth control, lower failure rates, and reduced maintenance costs. Consequently, it has demonstrated strong development potential and wide applicability in modern marine propulsion.

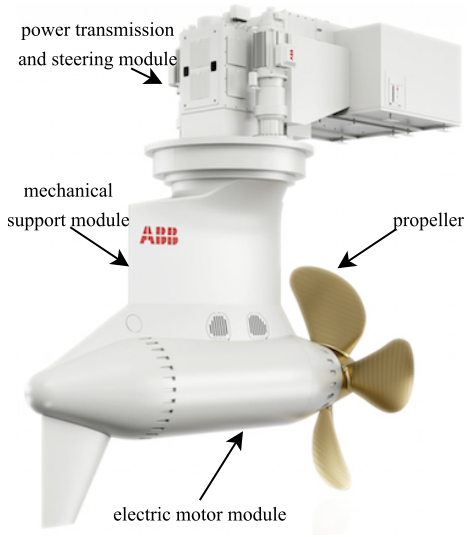

FIGURE 3. Pod propulsion device diagram.

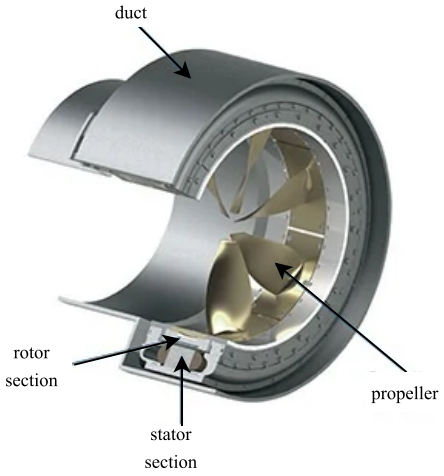

FIGURE 4. Diagram of a rim-driven thruster structure.

The rim-driven thruster integrates the motor rotor and propeller blades into a single structure, eliminating the conventional in-hull propulsion shafting and sealing systems [4]. Power is transmitted directly through the electrical energy, thereby requiring almost no space within the hull. As illustrated in Fig. 4, the rim-driven thruster primarily consists of propeller blades, a motor rotor, a multi-pole stator, water-lubricated bearings, and a ducted outer casing.

Since the rotational center of the propeller blades is hollow, two thrust bearings are mounted on both sides of the thruster. In addition, another configuration known as a hub-type rim-driven thruster was developed. Based on the shaftless rim-driven design, this configuration introduces an additional propeller hub at the rotational center, which is connected to the stator through guide vanes, as illustrated in Fig. 5.

1.3. Paper Motivation and Contribution

From the above overview of marine propulsion systems, several development trends can be identified:

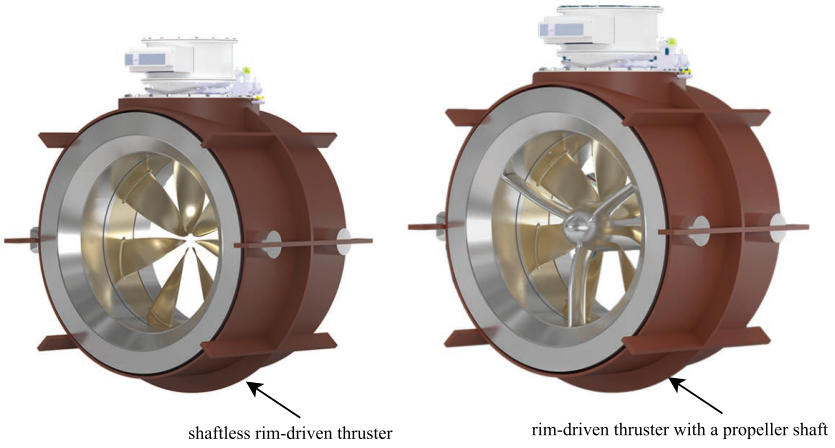

FIGURE 5. Rim-driven thruster device diagram.

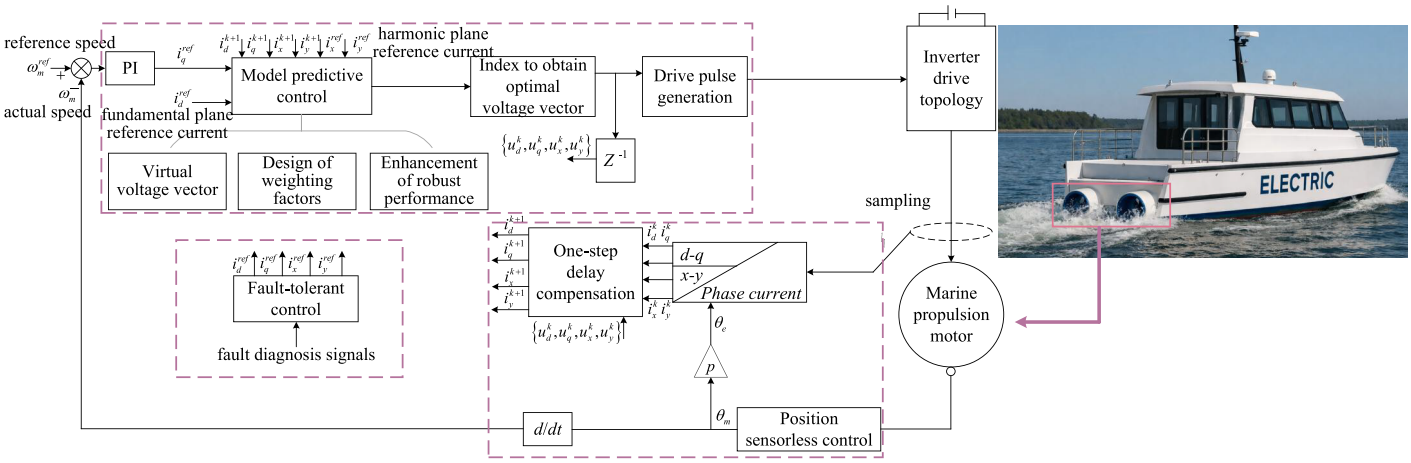

FIGURE 6. Framework of advanced control technologies for marine propulsion motors.

(1) Electric motors are gradually replacing traditional diesel engines as the primary source of propulsion power.

(2) Integrated direct-drive configurations are increasingly replacing the conventional gear-driven systems.

This indicates that the electric motor system will become the core component in the development and realization of high-performance green ships. As the central actuator of the entire vessel's propulsion system, its control strategy plays a crucial role in achieving both high performance and high reliability. In terms of performance, two primary objectives can be identified: (a) low vibration characteristics; and (b) strong dynamic tracking capability. Regarding reliability, the focus is mainly on two aspects: (a) fault-tolerant capability under motor or inverter faults; and (b) fault tolerance under position sensor malfunctions.

Based on the aforementioned primary objectives of marine propulsion motors, this study reviews research progress in advanced control strategies for marine propulsion motors over the past decade. The review is organized into three main themes: Section 3 focuses on high-performance control strategies, and Sections 4 and 5 address high-reliability control strategies. In particular, Section 6 discusses cutting-edge technologies for applying machine learning to marine propulsion motor systems.

Fig. 6 illustrates the overall framework of the advanced control techniques for marine propulsion motors reviewed in this paper. From Fig. 6, the interconnections among the three reviewed subtopics can be more clearly observed.

2. MOTOR TYPES AND DRIVE TOPOLOGIES

Three-phase motors have been widely used in various industrial applications. However, under extreme operating conditions, a phase loss in a three-phase motor can distort the magnetic field distribution within the motor, causing it to stall and potentially jeopardizing system safety. Compared with three-phase motors, multiphase motors have more winding phases, which increases their degrees of freedom. Consequently, without altering the inverter structure, multiphase motors can safely operate under fault conditions by simply adjusting the control strategy, thereby demonstrating a superior fault-tolerant capability. In addition, multiphase motors offer other advantages, such as reduced torque ripple and the ability to deliver high power even at low voltages, making them well suited for marine electric propulsion systems. The following provides a brief overview of motors with various phase numbers, including three-phase, five-phase, six-phase, nine-phase, and twelve-phase machines,

as well as open-winding topologies with neutral point access. It should be noted that this study focuses on six-phase motors (including dual three-phase configurations), which are the most extensively studied and applied, and provides a detailed analysis and discussion of their characteristics.

In direct-drive marine propulsion, achieving very low speeds requires increasing pole pairs or reducing inverter frequency, as per $n = 60f(1 - s)/p$. Both reduce speed but involve trade-offs. More pole pairs allow low-speed operation at higher frequencies, avoiding inverter issues such as harmonics, torque ripple, and losses at very low frequencies, but increasing motor size, weight, and cost. A lower frequency keeps the motor compact, but below 5–10 Hz, it weakens the magnetic field, reduces the load capacity, raises harmonics and thermal stress, and risks reliability. Thus, the low-speed direct-drive design balances pole pairs, operating frequency, and system cost. An integrated motor-inverter approach is often used to select pole pairs based on the inverter's stable minimum frequency to optimize the efficiency, size, and reliability.

2.1. Motor Types

Within the scope of this review, two main types of motors are considered: induction motors and permanent magnet motors. An induction motor operates based on the principle of electromagnetic induction. Alternating current supplied by the grid generates a magnetic field, and the rotating magnetic field produced by the stator induces currents in the rotor, thereby producing torque to drive rotor rotation. Its advantages include low cost, high durability, and good self-starting capability. However, its drawbacks are relatively low efficiency and power factor, as well as a high starting current. A permanent magnet motor generates torque through the interaction between the rotating magnetic field produced by the stator and the permanent magnets on the rotor. The main difference from an induction motor lies in the excitation method: a permanent magnet motor does not require current in the rotor to produce a magnetic field, thereby reducing energy losses. Its advantages include high efficiency and power density, as well as relatively simple structure and maintenance. The drawbacks are higher cost, risk of demagnetization, and greater dependence on accurate rotor position information. Induction and permanent magnet motors each have distinct advantages and characteristics in the field of marine electrification. For applications that require high durability and strict cost control, induction motors are preferred. In contrast, for high-end vessels where high efficiency and power density are prioritized, and cost constraints are more flexible, permanent magnet motors are more suitable.

In addition to conventional podded and rim-driven permanent-magnet machines, doubly salient permanent-magnet (DSPM) and switched reluctance machines (SRMs) are gaining attention for direct-drive marine propulsion [5, 6]. Their high saliency, magnet-free rotors, and multi-tooth designs enable high torque at low speeds. Recent optimizations show that multi-phase DSPMs can achieve torque density comparable to PMSMs with less magnet use [5], while offering improved thermal stability and fault tolerance. Long-standing torque ripple issues are being effectively addressed through combined structural improvements, such as optimized tooth profiles, and advanced control techniques like adaptive torque-sharing functions (TSF), reducing ripple by over an order of magnitude in low-speed operation [6]. Table 1 summarizes the existing torque ripple suppression strategies [7], systematically comparing their control complexity, effectiveness, and computational burden, thereby supporting the selection of suitable schemes for various propulsion applications.

TABLE 1. Main torque ripple mitigation methods of SRMs.

Method	Complexity	Torque ripple	Computation
Harmonic injection	High	Medium	Medium
TSF	Low	Medium	Low
DTC	Medium	High	Low
MPTC	Low	Low	High

Based on the number of phases, motors can be classified into conventional three-phase motors and multiphase motors. The following presents commonly used winding configurations for marine electric propulsion systems. Fig. 7 illustrates the winding configurations with a neutral point for three-phase symmetric, five-phase symmetric, six-phase symmetric, six-phase asymmetric, nine-phase symmetric, and twelve-phase symmetric motors. Fig. 8 illustrates the winding configurations of the two dual three-phase motors with dual neutral points. Corresponding to Fig. 7, Fig. 9 illustrates the open-winding configurations of the motors with the neutral point disconnected. The only difference between the two is the presence or absence of a neutral point.

Table 2 summarizes the comparative results for 14 marine propulsion motors with different phase numbers and winding configurations, as shown in Fig. 9. It can be observed that designs adopting multiple neutral points or open-winding configurations can significantly enhance the inherent fault-tolerant capability of the motor, but at the cost of increased control complexity. Table 2 provides a useful reference for selecting propulsion motors for various application requirements, cost constraints, and power levels.

2.2. Drive Topologies

For each phase of the motor, there are three main inverter drive topologies. The first is the two-level half-bridge, which provides two switching states per phase: ON and OFF. The second is the three-level full-bridge, offering three switching states per phase: forward conduction, OFF, and reverse conduction. The third is the diode-clamped three-level topology, which also provides three switching states. The specific topologies are shown in Fig. 10. A greater number of switching states provides more control degrees of freedom; however, the choice of topology should consider the specific operating conditions, as switching losses cannot be neglected.

3. MODEL PREDICTIVE CONTROL FOR MOTORS

The tremendous computational capabilities of modern microprocessors have spurred research on various high-performance

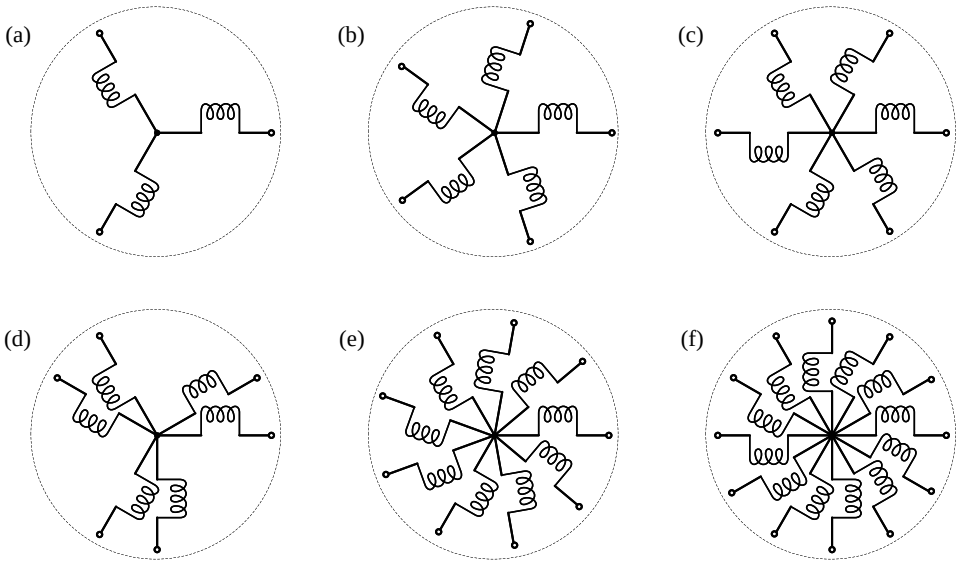

FIGURE 7. Diagram of neutral point motor winding distribution. (a) Three-phase symmetrical with neutral point. (b) Five-phase symmetrical with neutral point. (c) Six-phase symmetrical with neutral point. (d) Six-phase asymmetrical with neutral point. (e) Nine-phase symmetrical with neutral point. (f) Twelve-phase symmetrical with neutral point.

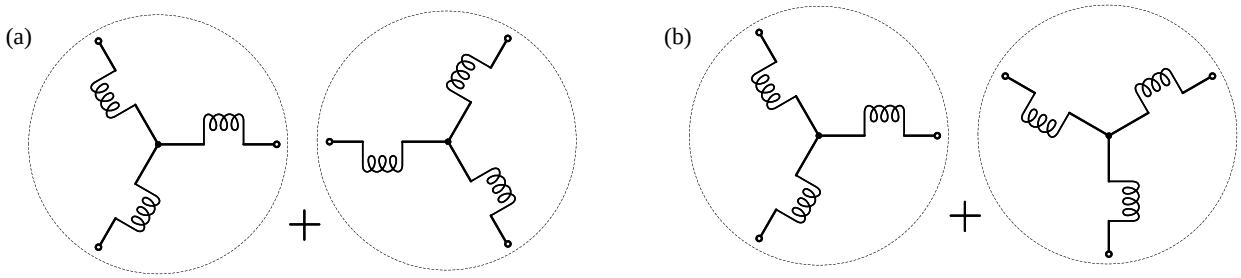

FIGURE 8. Double neutral point six-phase motor winding distribution diagram. (a) Six-phase symmetrical dual-neutral-point. (b) Six-phase asymmetrical dual-neutral-point.

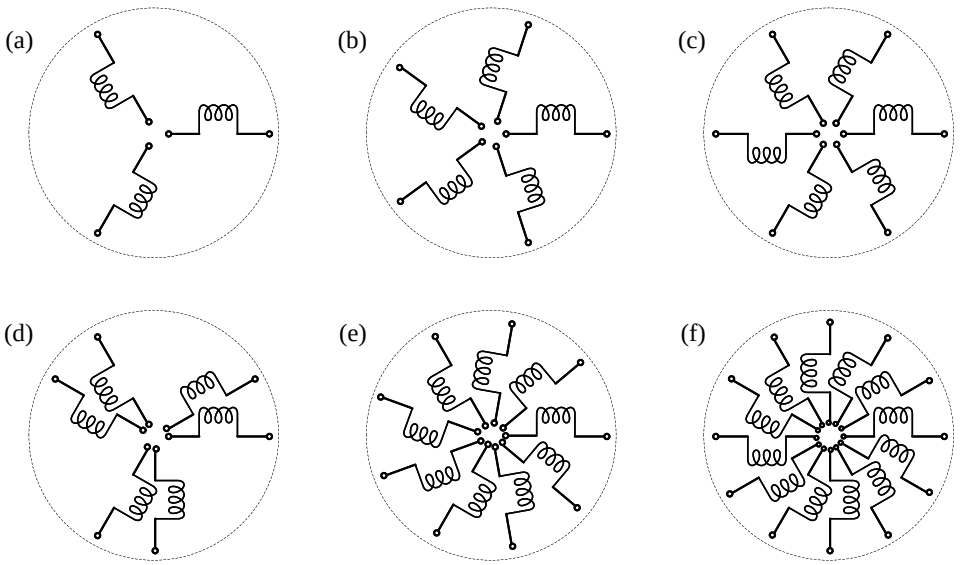

FIGURE 9. Diagram of open winding distribution of a motor without a neutral point. (a) Three-phase symmetrical open-end winding. (b) Five-phase symmetrical open-end winding. (c) Six-phase symmetrical open-end winding. (d) Six-phase asymmetrical open-end winding. (e) Nine-phase symmetrical open-end winding. (f) Twelve-phase symmetrical open-end winding.

TABLE 2. Comparison of motor phase number and winding structure configuration for marine propulsion applications.

Motor Type	Structure Complexity	Fault Tolerance	Control Complexity	Inverter Configuration	Suitability
3-phase symmetric with neutral	Low	Low	Low	3-leg inverter + neutral	Poor
5-phase symmetric with neutral [21]	Moderate	Medium	Moderate	5-leg inverter + neutral	Fair
6-phase symmetric with neutral	Moderate	High	Moderate–High	6-leg inverter + neutral	Good
6-phase asymmetric with neutral [28]	Moderate	Very High	High	6-leg inverter + neutral	Excellent
9-phase symmetric with neutral [34]	High	Very High	Very High	9-leg inverter + neutral	Good
12-phase symmetric with neutral [25]	Very High	Extremely High	Very High	12-leg inverter + neutral	Good
6-phase symmetric with dual neutral	Moderate–High	Very High	High	Dual 3-leg inverter (isolated neutrals)	Good
6-phase asymmetric with dual neutral [15]	High	Extremely High	Very High	Dual 3-leg inverter (isolated neutrals)	Excellent
3-phase open-end winding	Moderate	Medium	Moderate	Dual inverter per phase set	Fair
5-phase open-end winding [39]	Moderate–High	High	High	Dual inverter per phase set	Good
6-phase symmetric open-end winding [48]	High	Very High	Very High	Dual 3-leg inverters	Excellent
6-phase asymmetric open-end winding [32]	High	Extremely High	Very High	Dual 3-leg inverters	Excellent
9/12-phase symmetric open-end winding [38]	Very High	Extremely High	Extremely High	Dual multi-leg inverter	Good

TABLE 3. Current and future impact of control technology.

Control Technology	Current Impact	Future Impact
PID control	91%	78%
System Identification	65%	72%
Estimation and filtering	64%	63%
Model-predictive control	62%	85%
Process data analytics	51%	70%
Fault detection and identification	48%	78%
Decentralized and/or coordinated control	29%	54%
Robust control	26%	42%
Intelligent control	24%	59%
Discrete-event systems	24%	39%
Nonlinear control	21%	42%
Adaptive control	18%	44%
Repetitive control	12%	17%
Hybrid dynamical systems	11%	33%
Other advanced control technology	11%	25%
Game theory	5%	17%

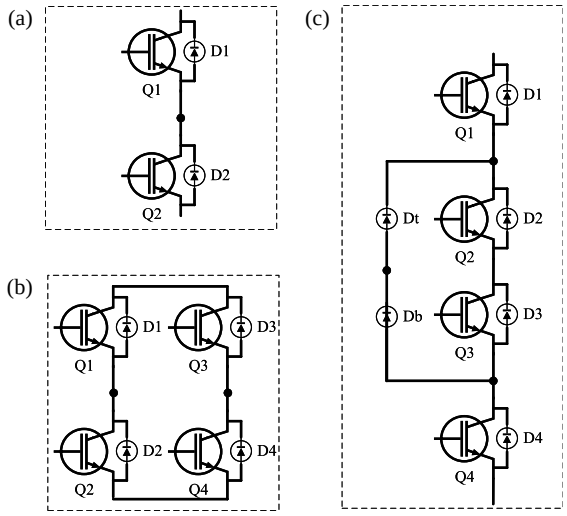

FIGURE 10. Schematic diagram of commonly used phase-driven topologies. (a) Half-bridge configuration for each phase (two-level). (b) Full-bridge configuration for each phase (H-bridge). (c) Half-bridge configuration for each phase (diode-clamped three-level).

drive control techniques, among which model predictive control (MPC) stands out. MPC offers rapid dynamic response, multi-objective, multi-variable, and multi-constraint control characteristics, along with the advantage of an intuitive and straightforward design [8, 9], making it a key strategy in the next generation of motor control. Furthermore, according to an industry survey in [10], MPC is expected to have a significant impact on future industrial applications. Its application to marine propulsion motor control aligns well with the stringent requirements for strong tracking performance and low vibration in marine electric drives. Table 3 presents the quantitative data of the influencing factors in model predictive control.

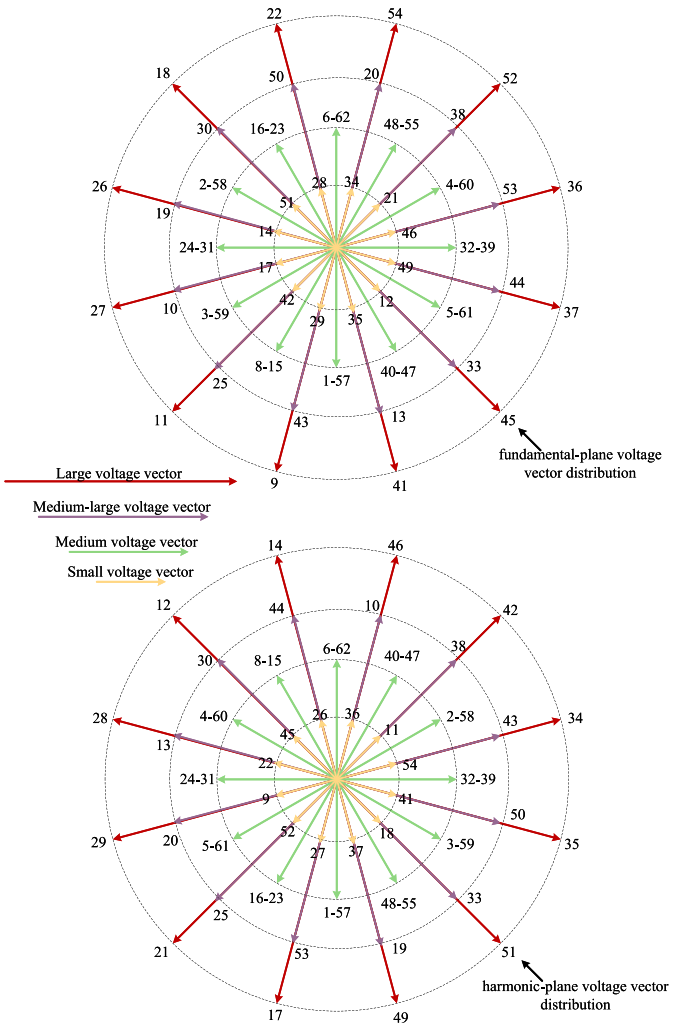

FIGURE 11. Voltage vector distribution in the $\alpha\beta$ and xy planes of a six-phase VSC.

3.1. Virtual Voltage Vector

Extending MPC to motors with more than three phases (i.e., multiphase motors) presents significant challenges. Not only does the computational complexity increase substantially, but additional degrees of freedom also require simultaneous current tracking within the harmonic subspace.

In [11], the authors simultaneously consider performance improvement in both fundamental and harmonic planes. Independent virtual voltage vectors are first used to ensure low circulating currents, and the optimal combination of two virtual voltage vectors enhances current tracking in the fundamental plane. This control strategy was implemented in an asymmetric six-phase induction motor. For a six-phase two-level voltage-source inverter (VSC), the distribution of the voltage vectors in the fundamental $\alpha\beta$ plane and harmonic xy plane is illustrated in Fig. 11.

As shown in Fig. 11, large voltage vectors with the same orientation in the $\alpha\beta$ plane are oriented oppositely in the xy plane, along with medium-large voltage vectors. Therefore, an appropriate combination of voltage vectors can be selected to cancel the generation of xy voltages, thereby eliminating the corresponding xy currents and copper losses. Specifically, a combination of one medium-large voltage vector and one large voltage vector can form a virtual voltage vector that ensures that the average voltage in the xy subplane is zero.

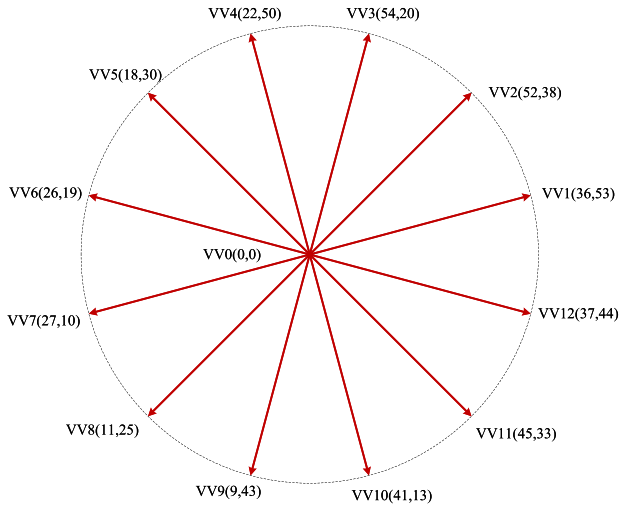

FIGURE 12. Virtual voltage vector distribution of a six-phase VSC.

To construct a virtual voltage vector, a medium-large voltage vector and a large voltage vector with the same phase must be applied within a single control period. As their orientations in the xy subplane are opposite, the respective application times can be calculated to ensure that the average voltage in the xy subplane is zero. The spatial distribution of the resulting virtual voltage vectors is shown in Fig. 12.

In [12], the authors also employ the virtual voltage vector technique. Similar to [4], it considers optimal dual-layer current tracking, while additionally analyzing the pulse-modulated switching sequences of all virtual voltage vectors to achieve simultaneous regulation in both the fundamental and harmonic subplanes. Other studies based on the virtual voltage vector method include [13] and [14], which are applied to six-phase permanent magnet synchronous motors, with [14] providing a brief analysis of overmodulation scenarios, [15] applying the method to a six-phase induction motor with a nine-switch topology, [16] employing duty-cycle-based virtual voltage vectors modulation, and [17] synthesizing new virtual voltage vectors using two adjacent virtual voltage vectors and a zero vector, enabling the output of arbitrary amplitude and phase in the fundamental plane.

3.2. Design of Weighting Factors

The tuning of weighting factors in the cost function of MPC is a challenging and non-negligible issue. Each controlled variable in the cost function, which is often expressed in different physical units, is associated with a weighting factor that reflects its relative importance. As the number of control objectives increases, the combination of weighting factors grows exponentially. Methods based on empirical trial-and-error or proportional scaling according to nominal values often fail to identify the optimal set. In this review, several approaches to address this problem are summarized.

TABLE 4. Main classification of weighting factors design and elimination methods in predictive control.

Main Category	Sub-method	Core idea and contribution	Reference
A. Model-structure-based Elimination			
Virtual vector and equivalent flux vector method	Low-complexity MPFC with dual virtual vectors	Uses dual virtual voltage vectors and lookup tables to reduce candidate set; converts torque and flux references into equivalent flux vector, eliminating weighting factors and reducing complexity.	[18]
Cost function redesign	Voltage vector error-based cost function	Designs cost function in terms of voltage vector error to eliminate weighting factors and simplify control.	[20], [21]
Model transformation	Dual-dq model-based control for six-phase IM	Replaces VSD with dual-dq transformation, giving equal importance to four current components, thus removing weighting factors.	[22]
B. Optimization-driven Determination			
Multi-objective optimization	MOPSO-based weighting factor design	Employs Pareto front in MOPSO to optimize weighting factors automatically, outperforming heuristic methods.	[19]
C. Hierarchical or Analytical Reduction			
Sequential or cascaded cost functions	Sequential and dual-plane predictive control	Introduces cascaded or sequential multi-stage cost functions (e.g., total torque and d-axis current), thereby eliminating weighting factors.	[23], [24]
Analytical reduction	Weight reduction via xy-plane voltage relation	Establishes analytical relationship between weighting coefficients and xy-plane voltage amplitude, reducing three coefficients to one.	[25]

In [18], the authors propose a low-complexity model predictive flux control (MPFC) method, which employs two sets of virtual vectors to reduce current harmonics and torque ripple. A predictive model is established, and a lookup table is developed to reduce the number of candidate voltage vectors, thereby lowering computational complexity. The torque and flux magnitude references are then transformed into an equivalent flux vector, avoiding the need for weighting factor tuning. Finally, both simulated and experimental results demonstrate that the proposed MPFC method outperforms three conventional weighted MPFC approaches under steady-state and transient conditions.

In [19], the authors propose a model predictive current control (MPCC) weighting factor optimization method based on a multi-objective particle swarm optimization (MOPSO) algorithm, utilizing the concept of the Pareto front. The test results indicate that the optimization performance of this approach is superior to that of the trial-and-error methods.

In [20], after obtaining precise reference voltage vectors, cleverly designs the cost function in terms of the voltage vector error, thereby eliminating the need for weighting coefficients and simplifying the control process. Similarly, in [21], the authors also adopt a cost function formulated based on the voltage tracking error.

In [22], the authors investigate the design of the weighting coefficients for six-phase induction motors. Unlike the previously mentioned solutions based on the virtual voltage vector concept, the proposed method is founded on a dual dq transformation model, which fundamentally alters the overall predictive structure compared with vector space decoupling (VSD) approaches. In this framework, the four resulting currents are considered of equal importance, thereby eliminating the need for weighting factor tuning.

In [23], the authors propose a simplified model predictive torque control (MPTC) algorithm for five-phase permanent magnet synchronous motors. By sequentially evaluating three cost functions to control the total torque and the d-axis current — referred to as sequential model predictive torque control — the weighting factors are effectively eliminated, partially addressing the challenge of the weighting factor design.

In [24], the authors similarly propose a cascaded cost function structure that eliminates weighting factors. The designed two-level cost functions correspond to the tracking errors of the orthogonal-axis currents in the fundamental plane and the harmonic plane, respectively.

In [25], the authors establish a relationship between the assignment of weighting factors and the voltage vector magnitudes in the xy harmonic plane, reducing the three original weighting factors in the cost function to one. This approach effectively alleviates the limitations associated with the difficulty of the weighting factor design.

Table 4 classifies and summarizes the weighting factor design methods used in model predictive, as proposed in the aforementioned studies. It can be observed that owing to the introduction of multi-plane modeling and virtual voltage vector techniques in marine propulsion motors, the design of weighting factors remains challenging and promising. Heuristic and intelligent optimization-based approaches have brought new vitality to this research area.

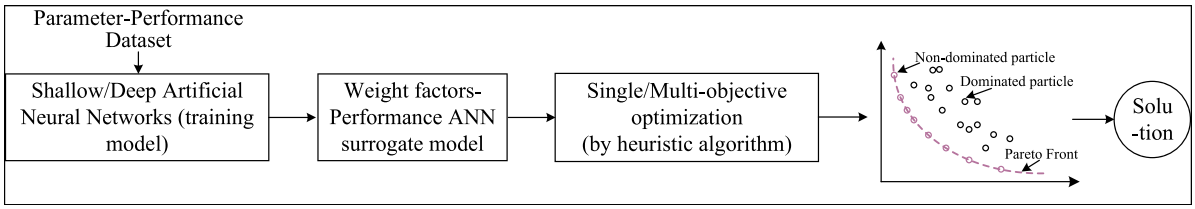

FIGURE 13. Process for optimizing weight factors using a machine learning surrogate model.

TABLE 5. Performance comparison: conventional and NSGA-II-optimized MPTC [26].

Method	T_{rip}	i_{thd}	f_{sw}
Conventional (No Load)	15.77%	6.32%	6.45 kHz
Optimized (No Load)	1.43%	5.13%	6.40 kHz
Conventional (With Load)	6.23%	6.18%	6.29 kHz
Optimized (With Load)	1.42%	5.12%	6.25 kHz

Moreover, the parameter design begins with criteria based on the control objectives. For example, in MPCC, equal weights are typically assigned to the q- and d-axis currents, whereas MPTC requires distinct weights for the flux and torque terms. For specific inverter topologies, secondary objectives — primarily harmonic and zero-sequence current suppression — must be incorporated into the cost function with suitable weights. Hardware constraints, such as penalties for switching actions and current limits, should also be integrated. Sensitivity analysis can be conducted by incrementally adjusting the weights with a defined step size while monitoring the performance indicators. However, traditional offline weight scanning is often time-consuming and limited in resolution. Insufficient analysis may weaken the effect of the weight factors. A more efficient and adaptive approach is proposed: First, parameter scanning is performed to generate a dataset mapping weight factors to performance metrics. This dataset is then used to train a surrogate model via machine learning, such as an artificial neural network. Finally, we employ single- or multi-objective optimization with this model to determine the optimal weight set, as illustrated in Fig. 13. The experimental performance comparison between the MPTC with multi-objective optimized weighting factors and the conventional approach is presented in Table 5.

3.3. Enhancement of Robust Performance

During motor operation, thermal effects and magnetic saturation can cause variations in resistance, flux linkage, and inductance. MPC, which relies heavily on accurate motor parameters, is therefore susceptible to performance degradation under parameter mismatches. This typically manifests as increased tracking errors and steady-state ripple, and in severe cases, the stability of the motor system may not be reliably ensured. Consequently, enhancing the robustness of motor parameter variations has become another critical issue to address. Several key technical approaches for achieving this are outlined below.

In [20], the authors address the parameter sensitivity issue in sector identification for obtaining reference voltage vectors and proposes a robust MPC incorporating a Luenberger observer. This approach compensates for the localized errors in the reference voltage vector positioning of six-phase permanent magnet synchronous motors. Studies demonstrate that employing the Luenberger observer effectively mitigates positioning errors and provides enhanced parameter robustness.

In [27], the authors propose a model-free predictive control method based on the current gradients. This approach not only minimizes currents in the xy harmonic plane using the virtual voltage vector concept, but also employs stored current gradients in the prediction step to compute the predicted current at the next instant, thereby avoiding the use of the motor model.

In [28], the authors propose a direct model predictive control (DMPC) scheme with an implicit modulator, aiming to minimize stator current errors and copper losses. To prevent performance degradation caused by parameter mismatches and model uncertainties, a disturbance observer based on a Kalman filter is implemented, effectively enhancing the robustness of the system.

In [29], the authors address the performance degradation caused by motor parameter mismatches and demonstrates that incorporating a prediction error compensation term into the predictive control model can eliminate steady-state current errors. To ensure system stability, the compensation term is activated only when steady-state errors occur between the reference and sampled currents owing to parameter mismatches or disturbances.

In [30], the authors propose a parameter identification method based on a sliding-mode observer to reduce the sensitivity of the motor parameters, thereby enabling the correction of mismatched parameters.

In [31], the authors propose a novel disturbance observer-redictive current control (DOB-PCC) strategy for six-phase PMSMs. The approach employs a disturbance observer (DOB) to estimate the total disturbance, compensating for parameter mismatch errors and unmodeled dynamics. The results demonstrate that the proposed strategy exhibits strong robustness against various parameter mismatch errors and dead-time values.

In [32], the authors proposed a model-free predictive current control (MFPCC) strategy for a fault-tolerant permanent magnet vernier rim-driven motor, where the control parameters were optimized using an artificial neural network. Fig. 14 illustrates the overall control framework, and Fig. 15 shows the experimental results that verify the robustness of the proposed

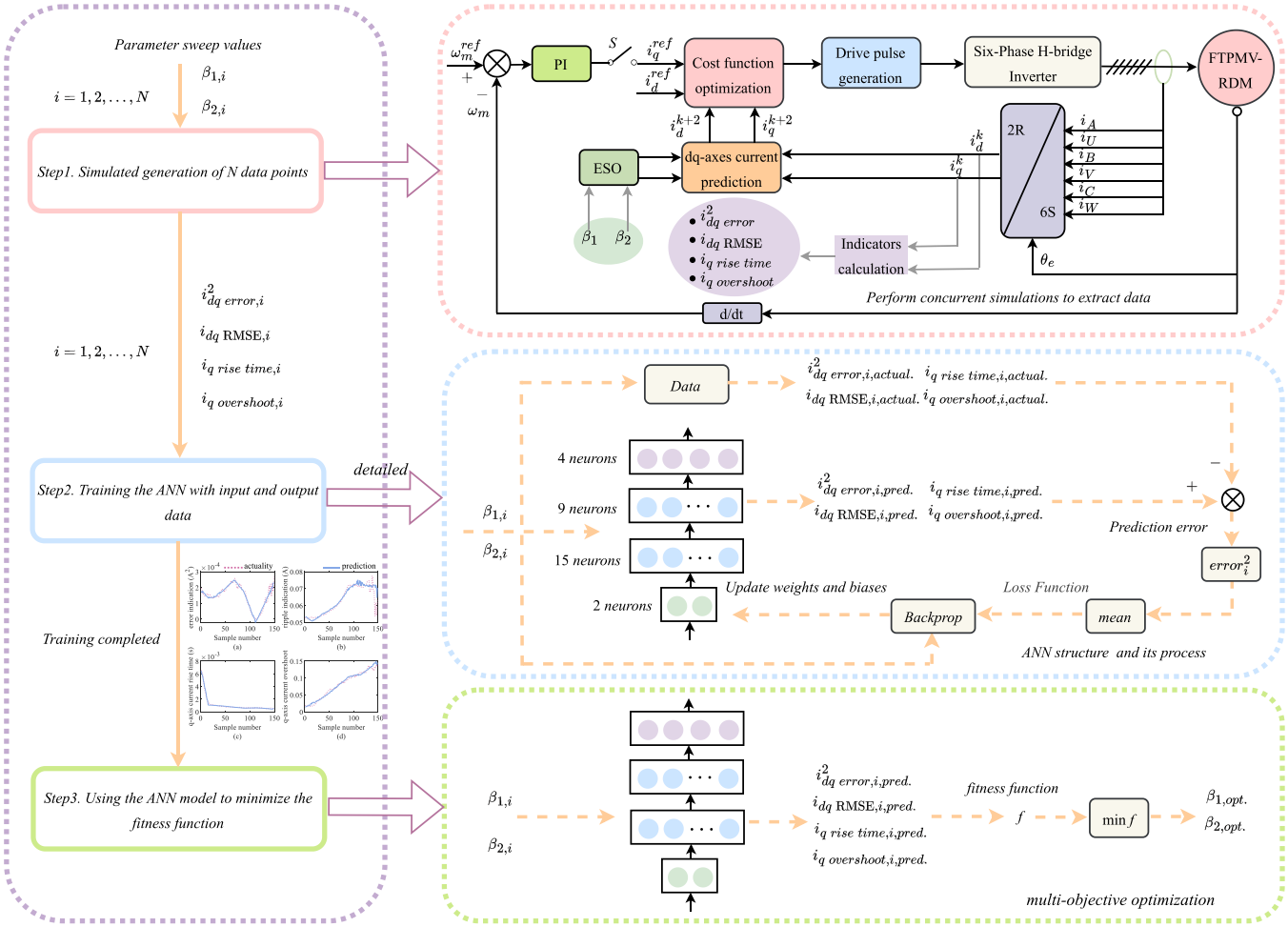

FIGURE 14. Model-free predictive current control for motors based on an artificial neural network in [32].

method. The results clearly demonstrate that machine learning-based approaches offer significant advantages.

Table 6 classifies and summarizes the methods proposed in the aforementioned studies for enhancing the robustness of model predictive control. It can be observed that model-free predictive control has gradually become a research hotspot, in which the novel machine learning-based optimization of extended state observers enables the algorithm to achieve both practicality and optimality.

4. FAULT-TOLERANT CONTROL FOR MOTORS

When operating for extended periods in the complex and variable marine environment, motors and their control systems inevitably experience faults. Severe vibrations or even motor stall can lead to significant, potentially incalculable risks to personnel safety and economic losses. Therefore, for marine propulsion systems, reliable and stable operation is a prerequisite for executing offshore missions. This necessitates that propulsion motors possess the capability to handle sudden faults, allowing continued fault-tolerant operation for a certain period to meet the requirements of high system reliability.

In [33], the authors investigate the operational conditions of a five-phase permanent magnet synchronous motor (PMSM) under normal operation, open-circuit or short-circuit faults in the windings, and inverter faults. Open-circuit faults include single-phase, two adjacent-phase, and two non-adjacent-phase disconnections, whereas short-circuit faults include single-phase-to-ground, adjacent-phase, and non-adjacent-phase short circuits. Inverter faults are considered the loss of switching capability of a single switch, which can only remain in the ON or OFF state. The results show a strong agreement between the proposed analytical model and finite element method simulations, demonstrating the general applicability of the model. A one-dimensional analytical approach is used to model the flux-current relationships in the PMSM with constant parameters.

In [34] and [35], the authors address torque ripple suppression under motor faults by replacing the proportional-integral (PI) controller in the rotor flux-oriented control (RFOC) current loops of multiphase induction motors with a fuzzy logic controller. Experimental results indicate that, compared with conventional RFOC with PI current control, fuzzy logic RFOC significantly improves the fault-tolerant capability of nine-phase

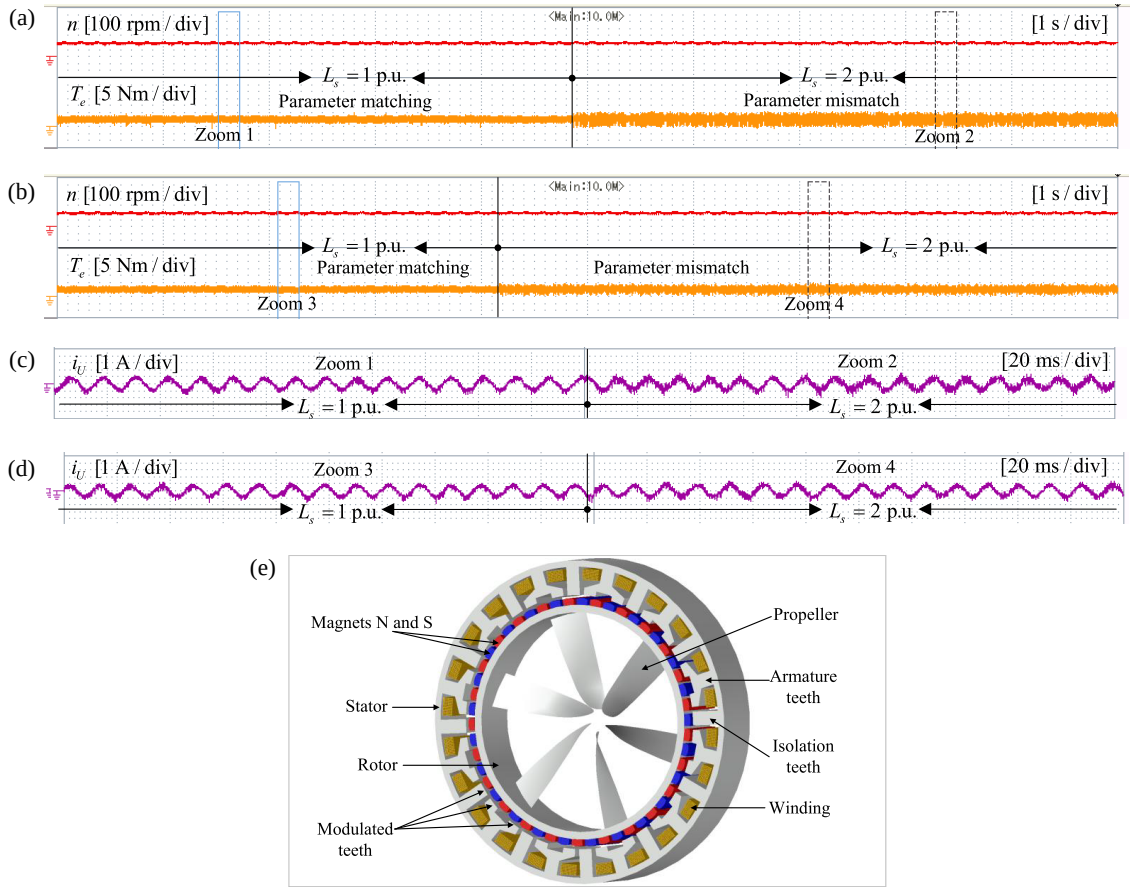

FIGURE 15. Robust control performance when inductance parameter mismath in [32]. (a) Speed and torque of traditional MBPCC. (b) Speed and torque of novel MFPCC. (c) Phase current of traditional MBPCC. (d) Phase current of novel MFPCC. (e) The prototype topology of FTPMV-RDM.

TABLE 6. Classification and summary of robust predictive control methods for motors.

Category	Method	Strengths	Weaknesses
Observer-based Robust MPC	Luenberger observer MPC [20]	Enhances sector localization accuracy and robustness to parameter drift.	Requires careful observer tuning and is sensitive to fast parameter variations.
	KF-based disturbance observer MPC [28]	Provides strong compensation for model mismatch and unmodeled disturbances.	Relies on accurate noise statistics and increases computational cost.
Disturbance/Error Compensation MPC	Prediction-error-compensated MPC [29]	Removes steady-state current errors through on-demand error correction.	Dependent on reliable error detection and limited transient improvement.
	DOB-based PCC [31]	Offers strong disturbance rejection and resilience to dead-time and parameter shifts.	Sensitive to measurement noise and requires bandwidth tuning.
Model-free/Data-driven MPC	Current-gradient MFPCC [27]	Avoids motor modeling and shows inherent robustness to parameter uncertainty.	Gradient estimation is noise-sensitive and may reduce steady-state accuracy.
	Sliding-mode identification MPC [30]	Online parameter self-identification improves adaptability and robustness.	Subject to chattering and requires filtering to suppress noise amplification.

drive systems under various fault conditions. In cases of single- or multi-phase open-circuit faults, switch failures, and combined faults, the fault-tolerant performance exceeds that of RFOC, although the steady-state performance under healthy operation is slightly inferior.

In [36], the authors introduce machine learning into motor fault-tolerant control, establishing an optimal single-phase open-circuit fault-tolerant control strategy for five-phase induction motors, which considers winding insulation reliability. Based on accelerated degradation data, insulation reliability models at different temperatures are constructed. A motor remaining useful life (RUL) prediction model is developed using Bayesian theory, along with a three-node lumped-parameter thermal network to predict winding temperatures under the

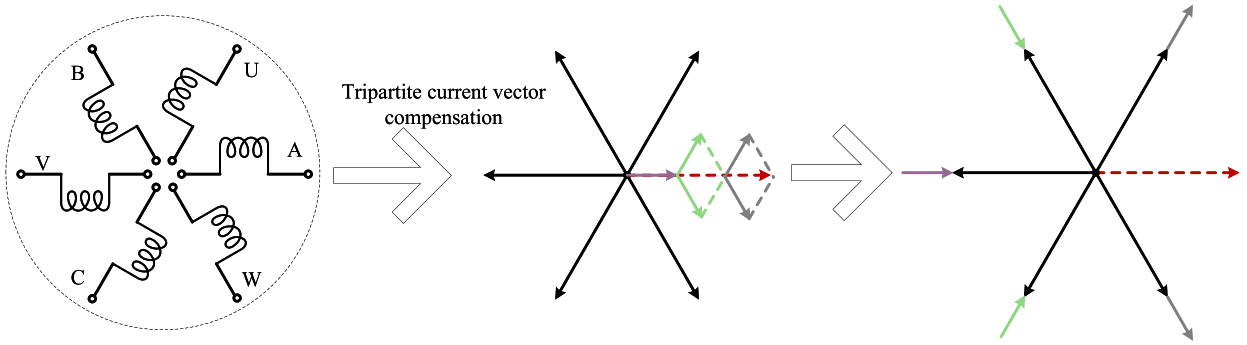

FIGURE 16. Schematic diagram of current vector compensation fault tolerance for single-phase open-circuit fault in a six-phase open-winding permanent magnet motor [48].

fault-tolerant strategy. An optimal fault-tolerant control model is also established, and the reconfigured fault-tolerant currents are calculated. According to the proposed algorithm, to maintain the synthesized stator magnetomotive force relative to the healthy condition, the currents in the remaining phases under fault must exhibit spatial mirror symmetry along the fault axis, ensuring that the instantaneous sum of all phase currents remains zero.

In [37] and [38], the authors compare the proposed method of reducing torque ripple under open-circuit faults by controlling the magnitude and phase angle of healthy-phase currents with three other fault-tolerant strategies. The first method controls a limited number of phases to reduce torque ripple, selecting control phases orthogonal to the fault phase to minimize the increase in the second-harmonic torque. The second method aligns the controlled phase with the direction of the second-harmonic torque component in the fault phase, compensating for ripple components to minimize the second-harmonic torque increase. The third method selects multiple healthy phases from the remaining healthy phases and applies equal control to minimize copper losses while keeping the sum of the second-harmonic torque components at zero. The test results show that all three methods effectively reduce torque ripple while maintaining possible torque output.

In [39], the authors focus on a five-phase PMSM, designing two sets of constraints: maintaining a constant stator flux and either equal phase current magnitudes or minimal winding copper losses. The computed results are constrained to remain within rated limits and transformed into a constrained nonlinear programming problem, solved via iterative optimization.

In [40] and [41], the authors propose a more novel fault-tolerant control method that achieves minimum torque ripple control by analyzing the steady-state symmetrical component model under motor faults. Reference [42] presents a fault-tolerant direct torque control (DTC) strategy, analyzing the impact of faults on the flux and torque. It combines direct torque control with different voltage vector selection tables before and after faults to implement fault tolerance using lookup tables. If other phases fail, two solutions are proposed: one is to store lookup tables for other fault conditions, and the other is to equivalently map the fault using fault symmetry to the current lookup table.

In [43] and [44], the authors propose fault-tolerant strategies from the perspective of the inverter topology by directly disconnecting faulty windings. In [43], a dual three-phase induction motor is modeled and controlled using indirect rotor flux-oriented control. Upon a fault, the faulty three-phase modular winding is directly disconnected, and reference currents for the remaining healthy phases are regenerated to ensure a steady-state performance. In [44], the authors consider a nine-phase permanent magnet synchronous motor with three sets of three-phase windings, each controlled by an H-bridge. In the event of an open-circuit fault, the entire set of symmetric three-phase windings containing the faulty phase is disconnected. To maintain the same output torque, the currents in the remaining healthy windings inevitably exceed their rated values. To ensure the safety of the motor system, under symmetric fault conditions, the effective values of the remaining phase currents must not exceed rated limits, necessitating derated operation.

In [45–47], the authors propose fault-tolerant control strategies for specific fault scenarios. Ref. [45] investigates a fault-tolerant control method for a three-phase permanent magnet synchronous motor (PMSM) under a particular power electronics fault, in which only one high-side switch and one low-side switch of two different phases operate in a standard three-phase six-switch inverter. The proposed control strategy assumes that the remaining switches fail in an open-circuit state while the corresponding anti-parallel diodes remain operational. A mathematical model for fault-mode operation is developed, and a control strategy for maintaining average torque is proposed. The strategy has been validated through simulations on a 50 kW marine propulsion motor. In [46], the authors address fault-tolerant control of a five-phase PMSM under inter-turn short-circuit (ITSC) faults. The fault mechanism of the five-phase PMSM is theoretically analyzed, revealing that a single-phase coil ITSC fault induces second- and fourth-harmonic speed fluctuations. A quasi-proportional composite integral (QPCI) controller is then proposed to suppress these fluctuations. The PI-QPCI controller consists of two QPCI controllers and one PI controller operating in parallel, providing high gain at the second- and fourth-harmonic frequencies, effectively mitigating speed oscillations. In [47], the authors focus on open-winding five-phase motors under semi-controlled inverter op-

TABLE 7. Classification and summary of fault-tolerant control methods for motors.

Category	Method	Core Idea	Strengths	Weaknesses
Fault Modeling	Analytical modeling [33]	Unified analytical modeling for inverter and phase faults.	Accurate fault prediction.	Limited transient representation.
Intelligent Control	Fuzzy-RFOC [34],[35]	Fuzzy replacement of PI for ripple suppression.	High adaptability.	Weaker healthy steady-state performance.
	ML-based FTC [36]	ML-based thermal and reliability-driven current redesign.	Balanced MMF & thermal safety.	High complexity, data-dependent.
Optimization/Reconfiguration	Current reconfiguration [37],[38]	Magnitude/phase optimization of healthy-phase currents.	Low torque ripple.	Parameter-dependent effectiveness.
	Nonlinear optimization [39]	Constrained optimization for constant flux and minimal loss.	Loss-minimized, limit-compliant.	Computationally heavy.
DTC/Symmetrical Component	Symmetrical-component FTC [40],[41]	Harmonic model for minimum torque ripple.	Simple, analytical.	Limited dynamic improvement.
	Fault-tolerant DTC [42]	Table switching for fault-aware vector selection.	Fast response.	Higher ripple, dead-time sensitive.
Topology/Special Strategies	Module isolation [43]	Disconnect faulty modules and reassign current.	High reliability.	Torque derating.
	Nine-phase modular FTC [44]	Isolate faulty groups via H-bridges.	Strong fault containment.	Higher cost/complexity.
	Extreme-fault inverter FTC [45]	Operates with minimal switches available.	Works under extreme faults.	Severely limited performance.
	ITSC & semi-controlled FTC [46],[47]	PI–QPCI ripple suppression + reconfiguration.	Effective harmonic mitigation.	Sensitive to parameter drift.

eration, proposing two fault-tolerant reconfiguration strategies that achieve satisfactory performance.

In addition to the commonly reported methods, a practical open-circuit fault-tolerant control technique has been developed for six-phase symmetric open-winding PMSMs, based on the concept of current vector compensation. When any phase experiences an open-circuit fault, the fault current magnitude is first divided into three equal parts [48]. Two mirror-symmetrical vectors are then combined to form one part, while the remaining part is synthesized individually with a healthy phase opposite to the faulty phase, as illustrated in Fig. 16. Fig. 17 shows the fault-tolerant control experimental results when an open-phase fault occurs in the permanent-magnet fault-tolerant rim-driven motor (FTPM-RDM). It can be observed that this method exhibits a fast dynamic response and excellent fault-tolerant capability.

Table 7 classifies and summarizes the fault-tolerant control methods proposed in the aforementioned studies. It can be observed that although a wide variety of fault-tolerant control strategies have been developed, the in-depth analysis of fault mechanisms, the efficient utilization of inverter topologies, and the flexible allocation of amplitude and phase among healthy phases remain enduring research themes.

5. POSITION SENSORLESS CONTROL OF MOTORS

Ships operate in complex and variable marine environments, subject to harsh conditions such as high temperature, high humidity, salt spray, and vibration. These factors make traditional motor systems that rely on position sensors susceptible to interference or damage, thereby increasing maintenance costs and the risk of system failure.

To address these challenges, position sensorless control techniques have emerged. By eliminating conventional position sensors and estimating motor states using electrical parameters such as currents and voltages, position sensorless control enables efficient and stable motor operation without relying on physical sensors. This approach not only enhances system reliability and reduces failure rates but also lowers costs and maintenance complexity, making it particularly suitable for maritime applications where reliability and spatial constraints are critical.

Next, we examine the application of position sensorless control algorithms in marine electric propulsion systems. The discussion begins with a comprehensive overview of the algorithm implementation, followed by a classification and analysis of their main features, suitable operating conditions, and the challenges they face.

In [49], the authors address the poor speed and position observation performance of peripheral direct-drive thruster permanent magnet synchronous motors by proposing a second-order sliding mode observer based on a super-twisting algorithm (STA-SMO). This approach effectively suppresses the chattering commonly observed in traditional algorithms while retaining the inherent robustness and insensitivity of conventional sliding mode observers. The estimated speed and rotor position angle can track the actual values in real time, maintaining high estimation accuracy. Fig. 18 presents a comparison of the block diagrams for the conventional SMO and the improved second-order STA-SMO employed in position sensorless control.

In [50], the authors investigate switched reluctance motors (SRMs) for marine propulsion. High-frequency pulse signals are injected during the non-conduction intervals, allowing the estimation of the non-conductive inductance and identification of its linear region. The upper and lower thresholds for the inductance are then set. The SRM's alignment position is determined, enabling rotor position estimation and conduction signal

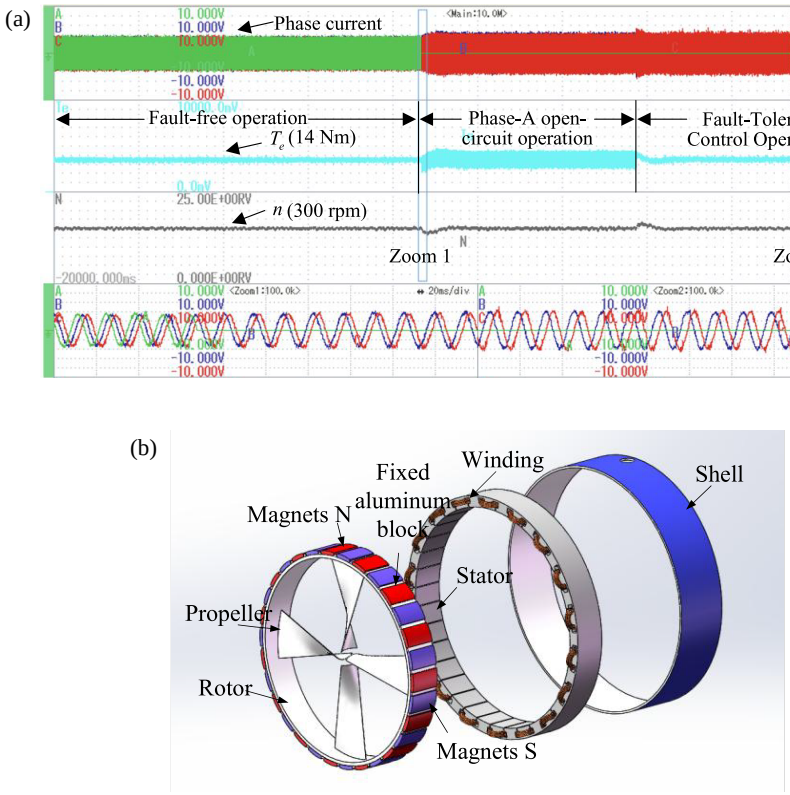

FIGURE 17. Experimental waveforms of the motor under phase open-circuit fault with current vector-based fault-tolerant control in [48]. (a) Current, torque, and speed waveforms. (b) The prototype topology of FTPM-RDM.

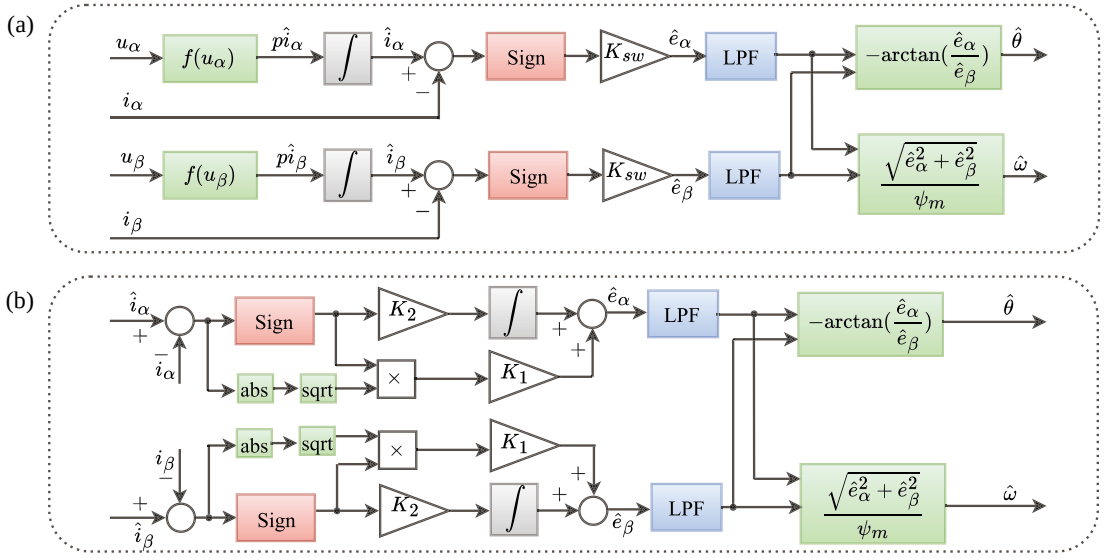

FIGURE 18. Control block diagram of the conventional SMO and improved STA-SMO presented in [49]. (a) SMO. (b) STA-SMO.

determination. The rotor angle and position are subsequently estimated based on the rotor position difference corresponding to the rising edge of the conduction signal.

In [51], the authors propose an adaptive observer for back electromotive force (EMF) and a speed extraction scheme based on an extended state observer (ESO). A sliding-mode adaptive observer estimates the extended EMF, which is then used in a cascaded ESO to extract the rotor speed. The results indicate that the ESO provides stable speed estimation and good dynamic response in low- and medium-speed ranges, outperforming conventional phase-locked loop (PLL) and NSFO methods.

In [52], the authors estimate motor speed and rotor position using the instantaneous values of motor voltage and current,

from which the amplitude and phase of the flux linkage vector are calculated. The use of integration can result in errors in flux calculation within the two-phase stationary reference frame. To address this, a low-pass filter is employed as an integrator to obtain the rotor position and speed. Comparative simulations were conducted under several frameworks: DTC/SVM (open-loop flux) and SVM (closed-loop flux).

In [53], the authors propose a position estimation algorithm based on a second-order sliding mode observer (SMO) combined with a PLL to meet the requirements of shipboard SPMSM drives. The study analyzes the effects of inverter nonlinearity and motor parameter variations on the estimation of rotor position from back EMF. A novel PLL incorporating a notch filter is utilized to effectively suppress AC periodic oscillations, and a gradient-descent-based extremum search control algorithm is applied to mitigate DC bias components.

In [54], the authors present a new terminal sliding mode observer (NFTSMO) designed in the two-phase stationary reference frame for rapid and accurate estimation of speed and position in dual three-phase PMSMs. The observer introduces a sliding surface to alleviate chattering issues inherent in conventional SMOs. Comparative analysis with traditional SMOs demonstrates that the proposed NFTSMO offers significant advantages, including superior speed tracking accuracy, more precise speed and position estimation, and enhanced stability, making it an ideal choice for marine propulsion drives.

In [55], the authors present a rotor position observer for permanent magnet hub motors based on an ESO to enhance the estimation accuracy of rotor position and speed. The ESO is employed to estimate the rotor's back EMF, from which rotor position and speed are derived using a PLL. On this basis, an Active Disturbance Rejection Controller (ADRC) is designed to handle nonlinear load disturbances caused by variations in propeller immersion depth.

In [56], the authors propose an enhanced fast terminal sliding mode observer (FTSMO) for position sensorless control of servo motors in marine propulsion systems. This method estimates speed and position in the two-phase rotating reference frame. Unlike back-EMF-based estimation approaches, it eliminates the need for a PLL, thereby reducing the computational burden on the control system and freeing designers from PLL parameter tuning challenges. To address the difficulty of speed estimation, particularly under reverse operation, an adaptive law is designed to directly estimate motor speed. Moreover, a novel terminal sliding surface is introduced to improve the reaching phase of the sliding mode, achieving faster convergence and higher position estimation accuracy compared with conventional terminal sliding mode methods. The finite-time convergence of the proposed estimation method is rigorously proven using Lyapunov theory, ensuring that the estimation error converges to zero within a finite time.

Model Reference Adaptive System (MRAS)-based sensorless control has been widely applied in PMSMs for marine propulsion. Unlike SMO, MRAS-based control does not suffer from chattering; however, it typically exhibits limited dynamic performance. In [57], the authors propose an improved rotor position estimation method based on conventional MRAS and a commonly used adaptive law. A novel rotor position adaptive law is introduced, which compensates for the estimated rotor angle, thereby enhancing the dynamic response without requiring an additional startup switching speed.

In [58], the authors address the specific characteristics of podded propulsion motors, which are fully enclosed and seawater-cooled, and proposes a position sensorless vector control system for SSP propulsion motors based on a strong tracking filter. The study also investigates the problem of state observation under abrupt load changes in harsh sea conditions. Simulation results demonstrate that by introducing a time-varying fading factor into the classical Kalman filter to adapt the predicted error covariance, the filter's ability to track sudden state changes is improved, yielding strong robustness and anti-disturbance performance. This approach satisfies the steady-state error requirements of podded propulsion systems and enhances the accuracy of state estimation.

In [59], the authors compare different observer methods and their performance for position sensorless control of large-ship propulsion PMSMs, providing practical guidance for selecting the most suitable observer technology. The observers analyzed include the SMO, MRAS, Luenberger Observer, and Extended Kalman Filter (EKF). The results indicate that the SMO exhibits good dynamic performance across both low and high-speed operating conditions.

All of the above methods are model-based position sensorless control techniques, which perform well in the medium-to-high speed range of the motor. However, at low speeds, the back EMF induced in the motor windings becomes very small. In the zero-speed region, the back EMF can nearly vanish, making it impossible to accurately measure and provide reliable information to the observer, resulting in unreliable rotor position estimation.

The high-frequency (HF) injection method is the primary technique used to estimate rotor position at zero and low speeds. It is based on either geometric saliency or saturation-induced saliency. While traditional HF signal injection strategies can effectively estimate rotor position and speed at low speeds, they also tend to induce significant torque ripple, which adversely affects the estimation accuracy of the position/speed in sensorless control algorithms and may compromise system stability.

Considering the characteristics of seven-phase PMSMs, the authors propose a new position sensorless control strategy applicable across the full speed range in [60]. At zero and low speeds, the high-frequency signal injection (HFSI) method is applied in the fifth-harmonic subspace to reduce torque ripple. At medium and high speeds, an SMO is employed in the fundamental wave space to estimate rotor position and speed. During transitions from low to medium/high speeds, the interaction between the two methods is effectively minimized. The proposed strategy achieves more accurate position and speed estimation while reducing torque ripple.

In [61], the authors focus on shipboard PMSMs and propose a rotor position estimation algorithm based on high-frequency pulsating voltage injection. The study analyzes the impact of inverter nonlinearity, current sampling errors, and HF injection signals on motor vibration. By embedding a notch filter,

TABLE 8. Summary of position sensorless control methods for marine propulsion motors.

Method	Basic Principle	Typical Improvement	Speed Range	Advantages	Limitations
Sliding-Mode Observer (SMO)	Based on back-EMF reconstruction using sliding-mode estimation	Super-twisting, non-singular fast terminal, adaptive SMO	Medium–high speed	Strong robustness, fast response, finite-time convergence	Chattering, degraded low-speed accuracy
Extended State Observer (ESO) / ADRC	Augments system state with disturbance term and compensates online	ESO + SMO / PLL combination for improved rejection	Full speed range	Effective disturbance estimation, strong adaptability	Parameter tuning complexity, sensitivity to noise
Model Reference Adaptive System (MRAS)	Compares reference and adjustable models to estimate rotor position	Improved reference model, adaptive gain design	Medium–high speed	Simple structure, low computational cost	Poor low-speed observability, parameter dependency
Kalman Filter (EKF/STKF)	State-space estimation with stochastic noise modeling	Strong-tracking, adaptive covariance update	Full speed range	High estimation accuracy, anti-noise capability	High computational cost, model mismatch sensitivity
High-Frequency Signal Injection (HFSI)	Injects HF voltage/current to extract saliency information	Rotating HF injection, demodulation optimization	Zero–low speed	Reliable zero-speed position estimation	Torque ripple, acoustic noise, extra hardware filtering
Hybrid Position Sensorless Control	Combines HFSI for low-speed and SMO/MRAS for high-speed	Seamless switching logic, adaptive weighting	Full speed range	Wide operation range, improved transition smoothness	Complex control logic, gain scheduling

the dominant harmonic components in the estimated rotor position are extracted, mitigating motor vibration. Additionally, a two-state Markov chain stochastic algorithm is introduced to randomize the injection frequency. This stochastic approach smooths the high-frequency current spectrum and reduces the peak electromagnetic vibration caused by the injected HF signals.

Table 8 classifies and summarizes the position sensorless control methods proposed in the aforementioned studies. It can be observed that, under medium- and high-speed operating conditions, various approaches such as the sliding-mode observer, extended state observer, model reference adaptive system, and extended Kalman filter have been employed. Among these, the sliding-mode observer exhibits the strongest robustness but faces greater challenges in parameter tuning. Furthermore, to achieve full-speed-range operation covering both zero/low-speed and medium/high-speed regions, most current studies adopt control schemes that switch algorithms according to the operating conditions.

A concise comparison of SMO, MRAS, and EKF highlights distinct trade-offs for marine propulsion drives. SMO delivers strong robustness and fast convergence but exhibits chattering and degraded low-speed accuracy under varying hydrodynamic loads. MRAS offers lightweight computation yet depends heavily on accurate parameters, limiting reliability over long voyages with temperature- and flux-driven drift. EKF achieves the highest precision and noise rejection but incurs high computational cost and is sensitive to model mismatch. Essentially, SMO prioritizes robustness; MRAS prioritizes simplicity; and EKF prioritizes accuracy, and its suitability hinges on the operating and economic constraints of the propulsion system.

6. FUTURE RESEARCH DIRECTIONS

6.1. Main Challenges

(1) Model Predictive Control (MPC): a) High sensitivity to parameters and limited robustness in the face of nonlinear marine propulsion dynamics. b) Complex multi-objective and multi-harmonic-plane optimization in multi-phase motors, making weight tuning difficult. c) Lack of effective analytical methods to balance torque, loss, ripple, and harmonics simultaneously.

(2) Fault-Tolerant Control (FTC): a) Complex post-fault coupling hinders multi-objective optimization (e.g., torque, loss, ripple). b) Most strategies are single-objective oriented and lack operational adaptability.

(3) Sensorless Control: a) No unified solution for the full speed range (zero to high speed). b) Poor low-speed performance and parameter sensitivity of conventional observers (SMO, MRAS, EKF). c) High-frequency injection improves zero-speed capability but introduces noise, ripple, and resonance risks.

6.2. Machine Learning Solutions and Experimental Validation

Machine learning can enhance motor robustness and fault tolerance. Key solutions, partially validated on a fault-tolerant permanent magnet vernier rim-driven motor (FTPMV-RDM), are outlined below.

(1) For MPC: a) Data-driven optimization of cost function weights. b) Machine learning-assisted observer tuning for improved robustness. c) Direct output of optimal voltage vectors by trained models.

(2) For FTC: a) Surrogate models to capture fault-condition nonlinearities. b) Multi-objective optimization for balancing

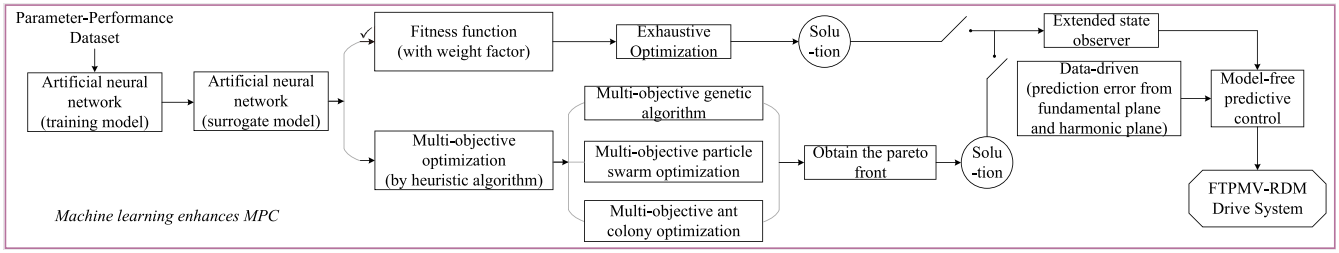

FIGURE 19. Schematic diagram of machine learning enhancing MPC.

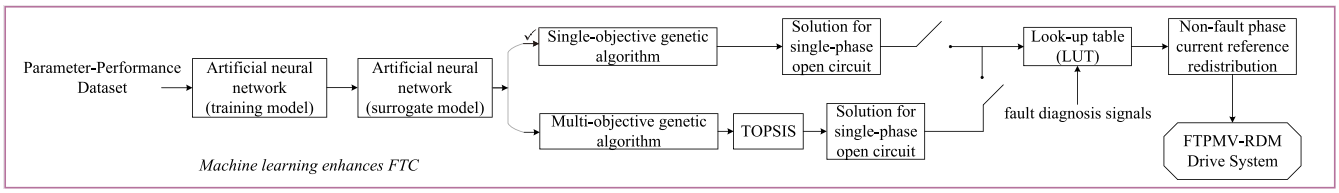

FIGURE 20. Schematic diagram of machine learning enhancing FTC.

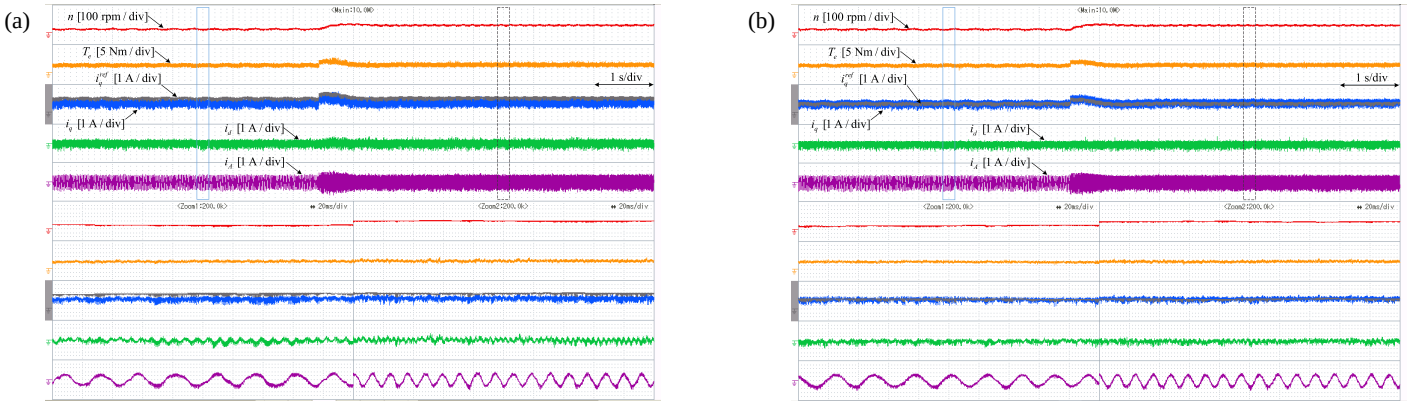

FIGURE 21. Experimental waveforms of the FTPMV-RDM under multi-parameter negative mismatch. (a) Model predictive current control. (b) Model-free predictive current control based on machine learning.

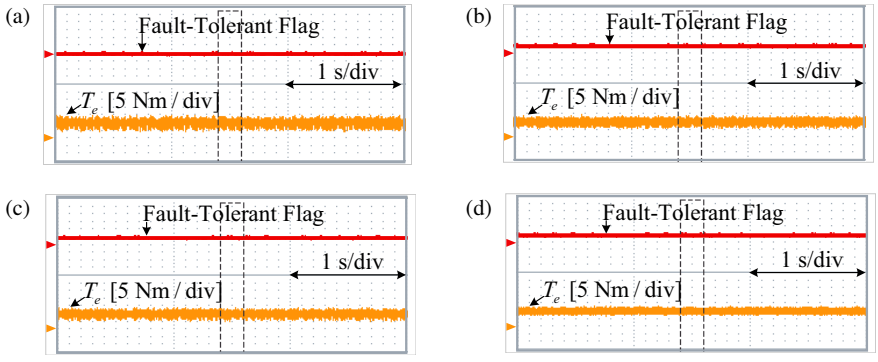

FIGURE 22. Experimental results of the FTPMV-RDM under open-circuit fault. (a) Fault and no fault-tolerant control. (b) FTC based on candidate vector set switching. (c) FTC based on current vector compensation. (d) FTC based on LUT with machine learning.

loss, torque, and ripple. c) Overcoming the single-objective limitation of traditional FTC.

(3) For Position Sensorless Control: a) Data-driven parameter identification for robust mid-high speed estimation. b) Design of observer parameters with higher stability. c) Low-noise zero-speed estimation via pseudo-random HF injection. d) ML-based switching logic for full speed-range stability.

(4) Experimental validation on FTPMV-RDM tests on a self-developed FTPMV-RDM included: a) ANN-based model-free

predictive control (robustness verification). b) Deep learning-based multi-objective FTC (performance under faults).

The FTPMV-RDM's high torque density and unique structure make it an ideal platform for advanced control strategy testing. Fig. 19 and Fig. 20 present two practical schemes for machine learning-enhanced MPC and FTC, tested on the FTPMV-RDM platform. Results in Fig. 21 and Fig. 22 confirm their satisfactory real-world performance. The online machine learning deployment can also be adapted, using either a lightweight or a lookup-table approach as required by the controller.

6.3. Machine Learning-Driven Industry Transformation

Future research may advance along three directions. First, further exploration of machine learning-driven adaptive MPC is needed to enable online parameter updates and automatic weight adjustment under complex operating conditions. Second, developing an intelligent multi-objective machine learning fault-tolerant control framework for marine propulsion applications can achieve global optimization of copper loss, torque, harmonics, and ripple. Third, a full-speed range position sensorless estimation method integrating physics-based models and data-driven approaches via machine learning can enhance stability and reliability in extreme conditions. Through these pathways, marine propulsion motor control is expected to progress toward greater robustness, efficiency, and intelligence.

7. CONCLUSION

This paper presents a comprehensive review of advanced control technologies for marine propulsion motors, with emphasis on model predictive control (MPC), fault-tolerant control (FTC), and position sensorless control. These methods constitute the core framework for achieving high performance and reliability in modern electric propulsion systems.

First, in the area of MPC, substantial progress has been made in multi-plane modeling and virtual voltage vector synthesis for multiphase permanent magnet motors. However, challenges remain, including strong parameter sensitivity, limited robustness under nonlinear marine operating conditions, and the difficulty of simultaneously optimizing torque, losses, ripple, and harmonics. These limitations underscore the necessity of more adaptive, data-driven MPC architectures.

Second, the existing FTC strategies, predominantly based on optimal current redistribution and H-bridge topology enhancement, provide effective post-fault operability. However, their single-objective nature and limited adaptability to various operating scenarios highlight the need for next-generation FTC approaches capable of multi-objective optimization under complex coupling conditions.

Third, position sensorless control techniques have achieved maturity in medium- and high-speed estimation, whereas zero- and low-speed operation still relies on high-frequency injection, which inevitably introduces noise, ripple, and potential mechanical resonance. A unified and robust full-speed-range solution is a key problem.

Machine learning is poised to address these challenges by enabling data-driven weight tuning and observer design for MPC, surrogate-model-based multi-objective optimization for FTC, machine learning-assisted parameter identification and switching logic for full-speed-range sensorless control. The integration of data-driven intelligence with physics-based modeling is expected to drive marine propulsion motor control toward greater robustness, efficiency, autonomy, and high performance.

ACKNOWLEDGEMENT

This work was supported by the National Natural Science Foundation of China under Grant 52377037, the Fundamental Research Funds for the Central Universities of China under Grant 3132023522.

REFERENCES

[1] Ouyang, W., *Performance Parameter Identification and Multi-Field Coupling Modeling of Marine Water-Lubricated Bearing*, Science Press, Beijing, China, 2023.

[2] Yan, X., X. Liang, W. Ouyang, Z. Liu, B. Liu, and J. Lan, "A review of progress and applications of ship shaft-less rim-driven thrusters," *Ocean Engineering*, Vol. 144, 142–156, 2017.

[3] Hansen, J. F. and F. Wendt, "History and state of the art in commercial electric ship propulsion, integrated power systems, and future trends," *Proceedings of the IEEE*, Vol. 103, No. 12, 2229–2242, 2015.

[4] Ma, R., J. Zhu, Q. Lin, and Y. Zhang, "Influence of winding distribution on fault tolerant performance in a fault-tolerant permanent magnet rim driven motor," *IEEE Access*, Vol. 7, 183 236–183 244, 2019.

[5] Guerroudj, C., J.-F. Charpentier, R. Saou, Y. L. Karnavas, N. Bracikowski, and M. E.-H. Zaïm, "Coil number impact on performance of 4-phase low speed toothed doubly salient permanent magnet motors," *Machines*, Vol. 9, No. 7, 137, 2021.

[6] Bekhouche, L., R. Saou, C. Guerroudj, A. Kouzou, and M. E.-H. Zaim, "Electromagnetic torque ripple minimization of slotted doubly-salient-permanent-magnet generator for wind turbine applications," *Progress In Electromagnetics Research M*, Vol. 83, 181–190, 2019.

[7] Sreeram, K., P. K. Preetha, J. Rodríguez-García, and C. Álvarez Bel, "A comprehensive review of torque and speed control strategies for switched reluctance motor drives," *CES Transactions on Electrical Machines and Systems*, Vol. 9, No. 1, 46–75, 2025.

[8] Rodriguez, J. and P. Cortes, *Predictive Control of Power Converters and Electrical Drives*, John Wiley & Sons, Hoboken, NJ, USA, 2012.

[9] Wallscheid, O., E. F. B. Ngoumtsa, and J. Böcker, "Hierarchical model predictive speed and current control of an induction machine drive with moving-horizon load torque estimator," in *2019 IEEE International Electric Machines & Drives Conference (IEMDC)*, 2188–2195, San Diego, CA, USA, 2019.

[10] Samad, T., M. Bauer, S. Bortoff, S. D. Cairano, L. Fagiano, P. F. Odgaard, R. R. Rhinehart, R. Sánchez-Peña, A. Serbezov, F. Ankersen, *et al.*, "Industry engagement with control research: Perspective and messages," *Annual Reviews in Control*, Vol. 49, 1–14, 2020.

[11] Aciego, J. J., I. G. Prieto, and M. J. Duran, "Model predictive control of six-phase induction motor drives using two virtual voltage vectors," *IEEE Journal of Emerging and Selected Topics*

in Power Electronics, Vol. 7, No. 1, 321–330, Mar. 2019.

[12] Luo, Y. and S. Niu, "Predictive current control for six-phase PMSM motor with multi-step synthesis based virtual vectors," *IEEE Transactions on Energy Conversion*, Vol. 38, No. 1, 134–146, Mar. 2023.

[13] Gonçalves, P. F. C., S. M. A. Cruz, and A. M. S. Mendes, "Multistage predictive current control based on virtual vectors for the reduction of current harmonics in six-phase PMSMs," *IEEE Transactions on Energy Conversion*, Vol. 36, No. 2, 1368–1377, Jun. 2021.

[14] Gonçalves, P. F. C., S. M. A. Cruz, and A. M. S. Mendes, "Predictive current control of six-phase permanent magnet synchronous machines with modulated virtual vectors," in *IECON 2019 — 45th Annual Conference of the IEEE Industrial Electronics Society*, 6229–6234, Lisbon, Portugal, 2019.

[15] Abdel-Moneim, M. G., W. E. Abdel-Azim, A. S. Abdel-Khalik, M. S. Hamad, and S. Ahmed, "Model predictive current control of nine-switch inverter-fed six-phase induction motor drives under healthy and fault scenarios," *IEEE Transactions on Transportation Electrification*, Vol. 10, No. 4, 10 125–10 135, Dec. 2024.

[16] Gonçalves, P. F. C., S. M. A. Cruz, and A. M. S. Mendes, "Predictive current control based on variable amplitude virtual vectors for six-phase permanent magnet synchronous machines," in *2019 IEEE International Conference on Industrial Technology (ICIT)*, 310–316, Melbourne, VIC, Australia, 2019.

[17] Wang, H., X. Wu, X. Zheng, and X. Yuan, "Model predictive current control of nine-phase open-end winding PMSMs with an online virtual vector synthesis strategy," *IEEE Transactions on Industrial Electronics*, Vol. 70, No. 3, 2199–2208, Mar. 2023.

[18] Luo, Y. and C. Liu, "A flux constrained predictive control for a six-phase PMSM motor with lower complexity," *IEEE Transactions on Industrial Electronics*, Vol. 66, No. 7, 5081–5093, Jul. 2019.

[19] Fretes, H., J. Rodas, J. Doval-Gandoy, V. Gomez, N. Gomez, M. Novak, J. Rodriguez, and T. Dragičević, "Pareto optimal weighting factor design of predictive current controller of a six-phase induction machine based on particle swarm optimization algorithm," *IEEE Journal of Emerging and Selected Topics in Power Electronics*, Vol. 10, No. 1, 207–219, Feb. 2022.

[20] Luo, Y., K. Yang, and Y. Zheng, "Luenberger observer-based model predictive control for six-phase PMSM motor with localization error compensation," *IEEE Transactions on Industrial Electronics*, Vol. 70, No. 11, 10 800–10 810, Nov. 2023.

[21] Liu, X., Z. Zhang, X. Gaol, Z. Li, J. Wang, L. Zhou, and R. Kennel, "Predictive current control of five phase permanent magnet motor with non-sinusoidal back-EMF," in *IECON 2018 — 44th Annual Conference of the IEEE Industrial Electronics Society*, 659–664, Washington, DC, USA, 2018.

[22] Mamdouh, M. and M. A. Abido, "Weighting factor elimination for predictive current control of asymmetric six phase induction motor," in *2020 IEEE International Conference on Environment and Electrical Engineering and 2020 IEEE Industrial and Commercial Power Systems Europe (EEEIC/I&CPS Europe)*, 1–6, Madrid, Spain, 2020.

[23] Liu, X., J. Wang, Z. Li, H. Zuo, L. Zhou, and R. Kennel, "Simplified predictive torque control of five phase permanent magnet motor with non-sinusoidal back-EMF," in *IECON 2018 — 44th Annual Conference of the IEEE Industrial Electronics Society*, 5855–5859, Washington, DC, USA, 2018.

[24] Feng, L., Z. Wang, J. Feng, and W. Song, "Cascaded model predictive control of six-phase permanent magnet synchronous motor with fault tolerant ability," *CES Transactions on Electrical Machines and Systems*, Vol. 7, No. 3, 311–319, Sep. 2023.

[25] Chen, B., J. Lv, X. Jiang, and Y. Zheng, "Model predictive control of a twelve-phase PMSM with simplified cost function," in *2019 22nd International Conference on Electrical Machines and Systems (ICEMS)*, 1–5, Harbin, China, 2019.

[26] Arshad, M. H., M. A. Abido, A. Salem, and A. H. Elsayed, "Weighting factors optimization of model predictive torque control of induction motor using NSGA-II with TOPSIS decision making," *IEEE Access*, Vol. 7, 177 595–177 606, 2019.

[27] Mamdouh, M. and M. A. Abido, "Current gradient based modified hysteresis controller for asymmetrical six-phase induction motor," *IEEE Journal of Emerging and Selected Topics in Power Electronics*, Vol. 12, No. 5, 5164–5175, Oct. 2024.

[28] Wu, Y., Z. Zhang, Q. Yang, W. Tian, P. Karamanakos, M. L. Heldwein, and R. Kennel, "A direct model predictive control strategy with an implicit modulator for six-phase PMSMs," *IEEE Journal of Emerging and Selected Topics in Power Electronics*, Vol. 11, No. 2, 1291–1304, Apr. 2023.

[29] Gonzalez-Prieto, A., I. Gonzalez-Prieto, O. Dordevic, J. J. Aciego, J. Montenegro, M. J. Duran, and M. U. Khan, "Memory-based model predictive control for parameter detuning in multiphase electric machines," *IEEE Transactions on Power Electronics*, Vol. 39, No. 2, 2546–2557, Feb. 2024.

[30] Song, X., H. Wang, X. Ma, X. Yuan, and X. Wu, "Robust model predictive current control for a nine-phase open-end winding PMSM with high computational efficiency," *IEEE Transactions on Power Electronics*, Vol. 38, No. 11, 13 933–13 943, Nov. 2023.

[31] Gonçalves, P. F. C., S. M. A. Cruz, and A. M. S. Mendes, "Disturbance observer based predictive current control of six-phase permanent magnet synchronous machines for the mitigation of steady-state errors and current harmonics," *IEEE Transactions on Industrial Electronics*, Vol. 69, No. 1, 130–140, Jan. 2022.

[32] Meng, Q. and J. Zhu, "Model-free predictive current control of FTPMV-RDM based on artificial neural network parameter optimization for ship electric drive," in *The 9th International Conference on Electromagnetic Field Problems and Applications (ICEF2025)*, 1–6, Harbin, China, Oct. 2025.

[33] Prieto, B., M. Martínez-Iturralde, I. Elosegui, and G. Artetxe, "A simple model for fault analysis of multiphase PMSM drives," in *2016 International Conference on Electrical Systems for Aircraft, Railway, Ship Propulsion and Road Vehicles & International Transportation Electrification Conference (ESARS-ITEC)*, 1–6, Toulouse, France, 2016.

[34] Liu, Z., Z. Zheng, and Y. Li, "Enhancing fault-tolerant ability of a nine-phase induction motor drive system using fuzzy logic current controllers," *IEEE Transactions on Energy Conversion*, Vol. 32, No. 2, 759–769, Jun. 2017.

[35] Liu, Z., Z. Zheng, Y. Li, and S. D. Sudhoff, "Fuzzy logic vector control design for fault-tolerant control of a 15-phase induction machine," in *2015 International Conference on Electrical Systems for Aircraft, Railway, Ship Propulsion and Road Vehicles (ESARS)*, 1–6, Aachen, Germany, 2015.

[36] Lin, Y., J. Zhang, Y. Fang, W. Liu, and F. Leng, "Fault-tolerant control strategy considering the insulation reliability of windings for five-phase induction motors," in *2023 26th International Conference on Electrical Machines and Systems (ICEMS)*, 1772–1777, Zhuhai, China, 2023.

[37] Park, H., T. Kim, and Y. Suh, "Fault-tolerant control methods for reduced torque ripple of multiphase BLDC motor drive system under open-circuit faults," *IEEE Transactions on Industry Applications*, Vol. 58, No. 6, 7275–7285, Nov.–Dec. 2022.

[38] Park, H., T. Kim, and Y. Suh, "Comparison of fault-tolerant control methods reducing torque ripple of multi-phase BLDC motor drive system under open-phase fault," in *2021 IEEE Energy Conversion Congress and Exposition (ECCE)*, 4987–4993, Vancouver, BC, Canada, 2021.

[39] Wei, Y., M. Qiao, and P. Zhu, "Fault-tolerant operation of five-phase permanent magnet synchronous motor with independent phase driving control," *CES Transactions on Electrical Machines and Systems*, Vol. 6, No. 1, 105–110, Mar. 2022.

[40] He, S., X. Sui, Z. Liu, M. Kang, D. Zhou, and F. Blaabjerg, "Torque ripple minimization of a five-phase induction motor under open-phase faults using symmetrical components," *IEEE Access*, Vol. 8, 114 675–114 691, 2020.

[41] He, S., X. Sui, D. Zhou, and F. Blaabjerg, "Torque ripple minimization of seven-phase induction motor under more-than-two-phase fault," in *2020 International Conference on Electrical Machines (ICEM)*, 2222–2228, Gothenburg, Sweden, 2020.

[42] Chikondra, B., U. R. Muduli, and R. K. Behera, "An improved open-phase fault-tolerant DTC technique for five-phase induction motor drive based on virtual vectors assessment," *IEEE Transactions on Industrial Electronics*, Vol. 68, No. 6, 4598–4609, Jun. 2021.

[43] Nounou, K., J. F. Charpentier, K. Marouani, M. Benbouzid, and A. Kheloui, "Fault-tolerant control of VSI driven double star induction machine for electric naval propulsion," in *2018 IEEE International Power Electronics and Application Conference and Exposition (PEAC)*, 1–6, Shenzhen, China, 2018.

[44] Zhai, Z., C. Li, M. Li, and X. Zheng, "Vector control of nine-phase permanent magnet synchronous motor under symmetrical fault condition for derating operation," in *2020 23rd International Conference on Electrical Machines and Systems (ICEMS)*, 2154–2157, Hamamatsu, Japan, 2020.

[45] Fernando, N., S. G. Jayasinghe, and A. T. Abkenar, "Marine propulsion PM motor control under inverter partial fault," in *2016 IEEE 2nd Annual Southern Power Electronics Conference (SPEC)*, 1–6, Auckland, New Zealand, 2016.

[46] Li, H., C. Wan, Y. Liu, and D. Zhang, "Fault-tolerant control strategy based on quasi-proportional complex integration controller for five-phase PMSM under coil inter-turn short circuit fault condition," in *2023 26th International Conference on Electrical Machines and Systems (ICEMS)*, 2210–2215, Zhuhai, China, 2023.

[47] Gong, S., Z. Liu, D. Jiang, W. Kong, and R. Qu, "Fault-tolerant reconfiguration control for the open-winding five-phase inverter under semi-controlled condition," in *2019 22nd International Conference on Electrical Machines and Systems (ICEMS)*, 1–4, Harbin, China, 2019.

[48] Wang, Z., "Vector control system of permanent magnet faulttolerant rim propulsion motor based on improved current hysteresis control," Master's thesis, Dalian Maritime University, Dalian, China, 2022.

[49] Yang, Z., X. Yan, W. Ouyang, H. Bai, and C. Ning, "Sensorless PMSM control algorithm for rim-driven thruster based on second-order sliding mode observer," in *2023 7th International Conference on Transportation Information and Safety (ICTIS)*, 244–249, Xi'an, China, 2023.

[50] Liu, H., Y. Zhao, Y. Fan, and J. Liu, "Torque predictive control based on an improved finite control set model of switched reluctance motor," in *2022 7th International Conference on Automation, Control and Robotics Engineering (CACRE)*, 126–131, Xi'an, China, 2022.

[51] Zhang, T., Z. Xu, J. Li, and H. Yan, "Enhanced speed extraction for salient PMSM sensorless drives based on a cascaded extended state observer," in *2018 IEEE International Conference on Electrical Systems for Aircraft, Railway, Ship Propulsion and Road Vehicles & International Transportation Electrification Conference (ESARS-ITEC)*, 1–6, Nottingham, UK, 2018.

[52] Ghosh, P. R., A. Das, and G. Bhuvaneswari, "Comparative analysis of sensorless DTC schemes for a synchronous reluctance motor drive," in *2018 IEEE International Conference on Power Electronics, Drives and Energy Systems (PEDES)*, 1–5, Chennai, India, 2018.

[53] He, Z., Z. Jia, L. Zhu, and F. Zhang, "Performance analysis of sliding mode position observer for marine SPMSM sensorless control," in *2018 IEEE International Power Electronics and Application Conference and Exposition (PEAC)*, 1–6, Shenzhen, China, 2018.

[54] Teymoori, V., H. Dastres, M. J. Kamper, R.-J. Wang, and N. Arish, "Sensorless control of DTP-PMSM ship-propulsion drives by using nonsingular fast terminal sliding mode observer," in *2023 26th International Conference on Electrical Machines and Systems (ICEMS)*, 4257–4262, Zhuhai, China, 2023.

[55] Zhang, S., T. Wang, and K. Wang, "Active disturbance rejection control for ship rim propulsion motors considering immersion depth of propeller," in *2023 26th International Conference on Electrical Machines and Systems (ICEMS)*, 410–415, Zhuhai, China, 2023.

[56] Teymoori, V., H. Dastres, M. J. Kamper, R.-J. Wang, and N. Arish, "Enhanced fast terminal sliding mode observer for wide-speed sensorless control of PM vernier ship propulsion machine drives," in *2023 International Aegean Conference on Electrical Machines and Power Electronics (ACEMP) & 2023 International Conference on Optimization of Electrical and Electronic Equipment (OPTIM)*, 1–7, Istanbul, Turkiye, 2023.

[57] Zhu, L., Z. Song, and Y. Zou, "Dynamic performance improvement of MRAS based sensorless control for permanent magnet synchronous machines," in *2023 26th International Conference on Electrical Machines and Systems (ICEMS)*, 421–425, Zhuhai, China, 2023.

[58] Yao, W.-L., Y. Liu, Z.-F. Yin, D. Zeng, and H.-Y. Li, "Speed sensorless vector control of marine podded propulsion motor based on strong track filter," in *The 27th Chinese Control and Decision Conference (2015 CCDC)*, 1882–1887, Qingdao, China, 2015.

[59] Tymoori, V., M. J. Kamper, R.-J. Wang, and G. Garner, "Comparison of sensorless control methods of PMSM ship propulsion drives," in *2023 International Conference on Electrical, Computer and Energy Technologies (ICECET)*, 1–7, Cape Town, South Africa, 2023.

[60] Wang, X., J. Gong, Y. Huang, E. Semail, N. Nguyen, and L. Peng, "High quality sensorless control strategy for seven-phase PMSM in full speed range," in *2023 26th International Conference on Electrical Machines and Systems (ICEMS)*, 3192–3197, Zhuhai, China, 2023.

[61] Yin, C. and Z. He, "Vibration reduction of marine permanent magnet propulsion motor without position sensor," in *2022 IEEE 10th Joint International Information Technology and Artificial Intelligence Conference (ITAIC)*, Vol. 10, 317–322, Chongqing, China, 2022.